國 立 交 通 大 學

電機與控制工程學系

碩 士 論 文

以 FPGA 為基礎之

自主性智慧型巡航控制系統設計

Design of an FPGA-based

Autonomy Intelligent Cruise Control System

研 究 生：張岑瑋

指導教授：吳炳飛 教授

中 華 民 國 九 十 五 年 七 月

以 FPGA 為基礎之自主性智慧型巡航控制系統設計

Design of an FPGA-based

Autonomy Intelligent Cruise Control System

研 究 生：張岑瑋　　　　　Student：Tsen-Wei Chang

指導教授：吳炳飛　　　　　Advisor：Bing-Fei Wu

國 立 交 通 大 學

電 機 與 控 制 工 程 學 系

碩 士 論 文

A Thesis

Submitted to Department of Electrical and Control Engineering

College of Electrical and Computer Engineering

National Chiao Tung University

in partial Fulfillment of the Requirements

for the Degree of Master

in

Electrical and Control Engineering

June 2006

Hsinchu, Taiwan, Republic of China

中華民國九十五年七月

以 FPGA 為基礎之
自主性智慧型巡航控制系統設計

學生：張岑瑋　　　　　　　　　　　　　　指導教授：吳炳飛

國立交通大學 電機與控制工程學系 碩士班

摘　　要

　　在智慧型運輸系統中的先進車輛控制與安全系統裡，適應性巡航控制系統扮演著一個相當重要的角色，例如減輕駕駛人負擔、輔助駕駛以及提高行車安全性。本論文的目標即在於研發高速縱向動態系統的主動式控制。

　　在這篇論文中，首先介紹我們所設計之適應性巡航控制系統的模式、目標以及基本理論。以此為背景，我們設計一個階層式的控制器。當駕駛人啟動控制系統後，假使前方無車，我們將會自動的定速行駛；假使前方有車，則可以依照駕駛者的需求，來決定安全行駛模式。

　　透過實驗車的建置，並經由實際道路之測試來驗證我們所需要的控制目標，最後將控制器實現在 FPGA 平台上。一般的巡航控制系統大部分是實現在車用電腦上。在此篇論文裡，我們雖然使用了在開發上會較為困難的 FPGA 平台，但是實驗過程驗證了它可以取代在車用電腦上之行車控制器。此控制方式不僅提供一個安全的行車方式，而且比一般車用電腦更加節省經費以及空間，適合作為一個車用控制器。

Design of an FPGA-based
Autonomy Intelligent Adaptive Cruise Control

Student：Tsen-Wei Chang   Advisors：Dr. Bing-Fei Wu

Department of Electrical and Control Engineering
National Chiao Tung University

ABSTRACT

Adaptive Cruise Control (ACC) System is an important part of the Advanced Vehicle Control and Safety System (AVCSS) in Intelligent Transportation Systems (ITS) such as drivers' burden lightening, driver assisting and safety driving. The target of this thesis is to develop an autonomy control system of a high-speed longitudinal motion control.

In this thesis, we first introduce modes, end and a basic theory of the designed adaptive cruise control system. In according with it, we design a hierarchical controller. After the driver starts the system, we can cruise at the pre-selected speed autonomously when there is no vehicle in front of us or select a driving mode according to the driver's need when there is a vehicle in front of us.

Through tests of the experimental vehicle, we reach our control goal according to road tests and implement it on an FPGA platform. In general, cruise control systems are realized on car computers. In this thesis, though it is more complex to develop with an FPGA we used. But we verify it that control rules on car computer can be implemented with an FPGA. Have represented a safe driving mode and it is not only smaller but also cheaper than a car computer. It is suitable for an automobile-used controller.

ACKNOWLEDGEMENTS

TABLE OF CONTENTS

LIST OF FIGURES

LIST OF TABLES

Chapter 1   Introduction

1.1   Motivation

According to statistics of Ministry of Transportation, at least three thousands people are suffered injuries in traffic accidents every year in Taiwan. However, most accidents were results of human oversights. Since many studies have shown that over 90 percent of highway accidents are occurred due to driver-related errors [1], the main initiative is to improve safety of the automation system interacted with the human driver. In order to improve the safe driving, intelligent transportation system (ITS) is usually used to solve this problem.

There is a board range of diverse technologies under the generic topic of ITS that holds the answer to many of the transportation problems. One of the applications of ITS is the providing of assistance to control some of vehicle elements, like the throttle pedal and consequently, the speed-control assistance. A cruise control (CC) system is a common application of these techniques. It consists of maintaining the vehicle speed at a driver pre-set speed. On the basis of CC, the adaptive cruise control (ACC) is also a common application. An ACC-equipped vehicle detects the presence of a preceding vehicle and measures the distance by using a forward looking sensor. It automatically adjusts the vehicle speed to keep a proper range when a preceding vehicle is detected. When no preceding vehicle is detected, it functions like a CC. This is achieved through a laser range finder, digital signal processor and a throttle controller.

Although ACC systems have been in market since 1995, it is still as an optional

device for luxury vehicles. One of the reasons is that ACC systems are not cheap. One of expensive components is the controller which may be a notebook or car computer. We want to design a chip to replace the controller and have the aid of semiconductor manufactures to cost down. And then ACC system could be popularized to par vehicle. In order to determine if it is feasible to replace the controller with a chip, we use FPGA to test and verify it. Besides we do our best to use not expensive sensors and popular chips and to grab the signal from vehicle itself by avoiding installing sensors on it.

1.2   Autonomy Adaptive Cruise Control system configuration and operation modes
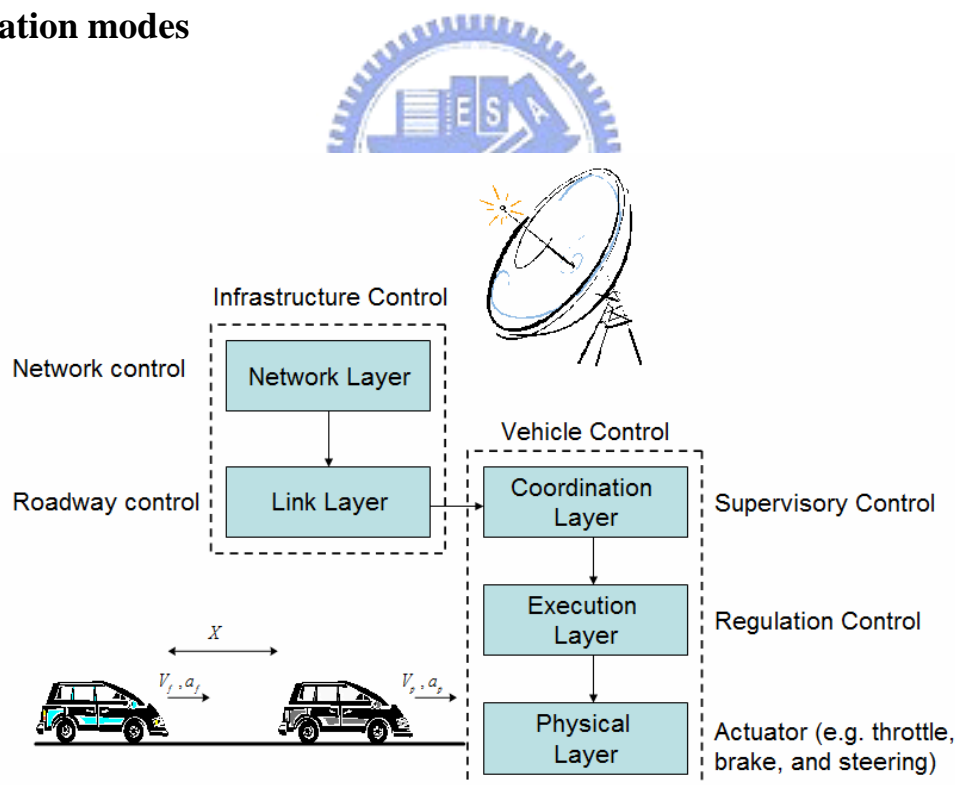
Figure 1-1 Hierarchical control structure for autonomy system

In terms of the general autonomy system design in vehicles, the complete hierarchical control structure is shown in Figure 1-1. The structure is composed of

different layers, among which the network and link layers are owned by the infrastructure, and the coordination, execution, and physical layers are constructed in the subject vehicle.

It has been proposed in [12] for the function of infrastructure control consisting the network and roadway control. The network control optimizes the traffic network and provides the desired traffic distributions to the link layer of the roadway control. By receiving the desired traffic density distributions from the network control, the roadway control issues the speed and headway commands to the subjected vehicle by using the roadside beacons or other communication devices connectable between the infrastructure and the vehicles.

The subject vehicle operating in the configuration of Figure 1-2 is equipped with the on-board control system that can respond to the commands of the roadway control and the driver. The on-board control system consists of the coordination and execution layers. In the coordination layer, the supervisory control communicates with the roadway control, other vehicles, and the driver, to recognize the desired operation mode of the vehicle following control. During different control modes, the supervisory issues the appropriate commands to the regulation control in the execution layer. The actuators in the physical layer, including throttle, brake, and steering wheel, are derived by the appropriate commands generated from the regulation control.

In this thesis, the coordination and the execution layer, by designing the architecture of the supervisory and the regulation control, respectively, are concentrated. The developed longitudinal motion control in the autonomy adaptive cruise control for vehicles can be generally used for several modes of following operations.

1.2.1 Intelligent cruise control mode

The objective of the intelligent cruise control (ICC) operating mode is to allow automatic vehicle following under the supervision of the driver. The driver sets the desired velocity and takes responsibility of steering and recognizing possible emergencies. In this case, the roadway can issue desired velocities to the driver by road signs.

The supervisory control receives the input of the desired velocity from the driver, and sends the appropriate velocity command to the regulation control to achieve the objective of the ICC mode.

1.2.2 Adaptive cruise control mode

In the adaptive cruise control (ACC) mode, the objective is to adapt the controlled vehicle velocity and maintain the safety distance to the preceding vehicle. The permitted headway time command can be sent from the roadway control or set by the driver. However, to take over the responsibility for emergencies in the ACC mode, the headway time is to be decided by the longitudinal control system rather than the driver.

Within this operation mode, the supervisory control should be able to communicate and respond to the roadway commands. Besides, the supervisory control could handle the communication with preceding vehicles in the same lane in addition to the tasks without vehicle-to-vehicle (v-v) communications. According to the desired headway time command, the supervisory control processes all the available

inputs and transmits the appropriate velocity command to the regulation control execution to guarantee collision-free of vehicle following process. Notably, the transition from automatic to manual control should not leave the driver out of safety handling.

1.2.3 Platoon control mode

To improve the capacity without affecting safety, the platoon control mode could be acted with the capability of communicating with the roadway control and other vehicles in the same lane. The distinction between the platoon control mode and the ACC mode is the decision of the headway distance. In platoon control mode, the headway distance between controlled vehicles is fixed and smaller, while the headway distance is adaptive in accordance with the safety headway time strategy in the ACC mode.

The desired headway distance should be sent from the roadway control. The supervisory control receives the operation command of the intra-platoon distance, and the desired velocity command is transmitted to the execution of the regulation control to achieve the objective of platoon control mode. Once the emergencies during the platoon process are recognized, or the platoon control mode is not suitable, the ACC mode will be chosen or taken over by the driver.

1.2.4 Selection logic of the operation mode

It is essential to consider different operation modes in the design of the autonomy

adaptive cruise control (AACC) in case that some vehicles are not provided with the communication devices to the infrastructure and nearby vehicles. The different operation modes in the AACC are recognized in terms of the handling authority between the driver, nearby vehicles, and the infrastructure facilities. In addition, to reduce workload of the driver, the logical way for determining the operation mode of the AACC should autonomously detect the presence of certain events.

The selection logic for the different operation modes is shown in Figure 1-2. While the AACC is activated, the supervisory control proceeds with the automatic selection of the operation mode. If once the valid target is detected during the controlling process, then the supervisory will choose the ACC or the platoon control mode dependent on the existence of the roadway control. Notably, here the valid target conforms to the following conditions:

1   The valid target is within the designated range based on the feasible field of the sensor, e.g., laser range finder, etc.

2   The velocity of the valid target is slower than the subject vehicle in the ICC mode.

The vehicle in front will not be considered as the valid target if either of these two conditions is not satisfied.

As shown in Figure 1-2, if the subject vehicle is cruising in the ICC mode, the desired velocity is commanded by the driver. In the ACC mode, the desired headway is inferred by the safety headway time strategy. As to the platoon control mode, the appropriate intra-space is determined from the roadway control. Unlike the ICC mode, the communication with other vehicles can be used in both ACC and platoon control mode to achieve more precise vehicle following control.

The selection logic scheme for different operation modes is constructed in the supervisory control. For each operation mode, the desired velocity V_d is filtered

against noise and passed to the regulation control to obtain the smooth response.
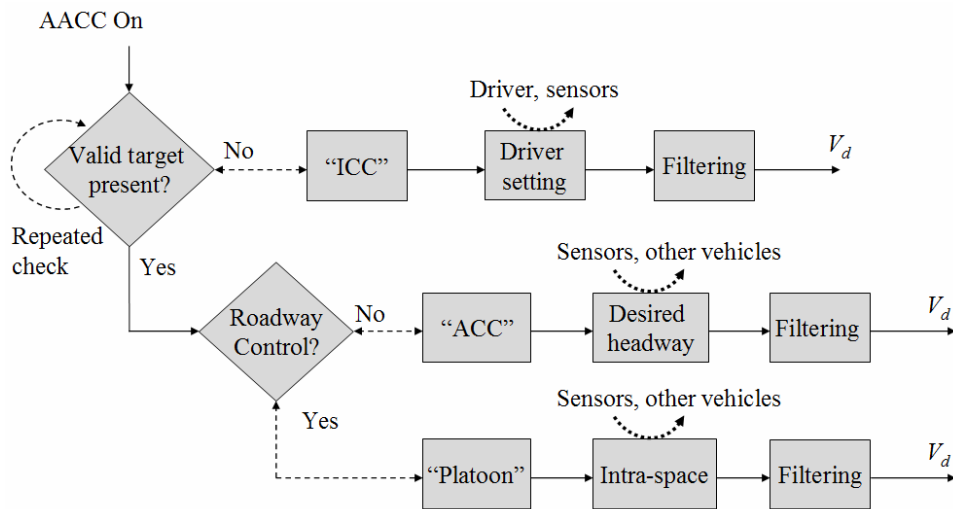
Figure 1-2 Operation mode selection logic

1.3 FPGA based controller

A Field Programmable Gate Array (FPGA), which is made up of Combinational Logic Blocks (CLB), is a digital integrated circuit that can be programmed to do any type of digital functions. These blocks are made up of an array of digital AND, OR and INVERT gates. The CLBs are arranged in an array to implement different design. Each block is planed to perform a logic function that can be interconnected, so that the complete logic function can be implemented.

There are many advantages of an FPGA over a microprocessor chip for our systems:

(1) An FPGA has the ability to be reprogrammed very easily and quickly. Therefore FPGA is suitable for fast implementation and quick hardware verification. As compared to the dedicated fuzzy hardware, FPGA based system is more flexible

7

than fuzzy chips. We can make changes if the design is incorrect. They can be easily reconfigured with new design. Hence it is often used to be a prototype chip to verify the function is correct or not.

(2) An FPGA is programmed just using support software and a download cable connected to a host computer. Once they are programmed, they can be disconnected from the computer and will retain their functionality until the power is removed from the chip. A Read Only Memory (ROM) type of a chip that is connected to the FPGA programmable inputs can also program the FPGA upon power-up. This means that when a board is in place in a remote location, the chip can keep running while the designer updates the design back at a lab. Once the designer updates the design he or she can program another ROM chip, take it to the site and replace the old ROM chip. The next power-up the chip will be reprogrammed to the new design.

(3) An FPGA is described or modeled using Hardware Description Languages like Very High Speed Integrated Circuit Hardware Description Language (VHDL), Verilog, etc and verified by simulation. VHDL is now one of the most popular standard HDLs and can be used to describe the behavior or structure of the digital system.

The thesis presents the design and implementation of a digital fuzzy logic controller on an FPGA using VHDL.

1.4   Brief sketch of contents

The thesis is organized as follows: Overall structure of vehicle longitudinal control system is presented in Chapter 2. In Chapter 3, we will discuss the peripheral interface of the system. In Chapter 4, we introduce the design background. The

experimental results are given in Chapter 5. Finally, conclusions are described in Chapter 6.

Chapter 2　Overall Structure

Figure 2-1 shows the basic function that it will compute the safe distance and keep the suitable velocity of the following vehicle by a forward looking sensor and throttle control.
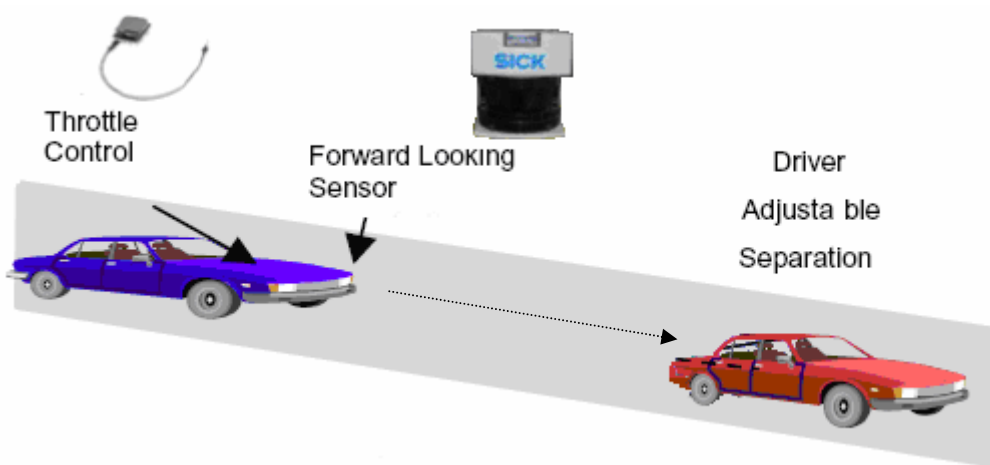
Figure 2-1 Sketch map of adaptive cruise control

2.1　Driving mode

Figure 2-2 shows the AUTO-IACC system possessed of three modes: intelligent cruise control (ICC), adaptive cruise control (ACC) and platoon control. When there are no vehicles or obstacles in the same lane, the ICC system works like a cruise control system that maintains a pre-selected speed, if a vehicle with slow speed or an obstacle is ahead in the same lane, the ACC system or the platoon system automatically will reduce its speed and maintain the safety distance.
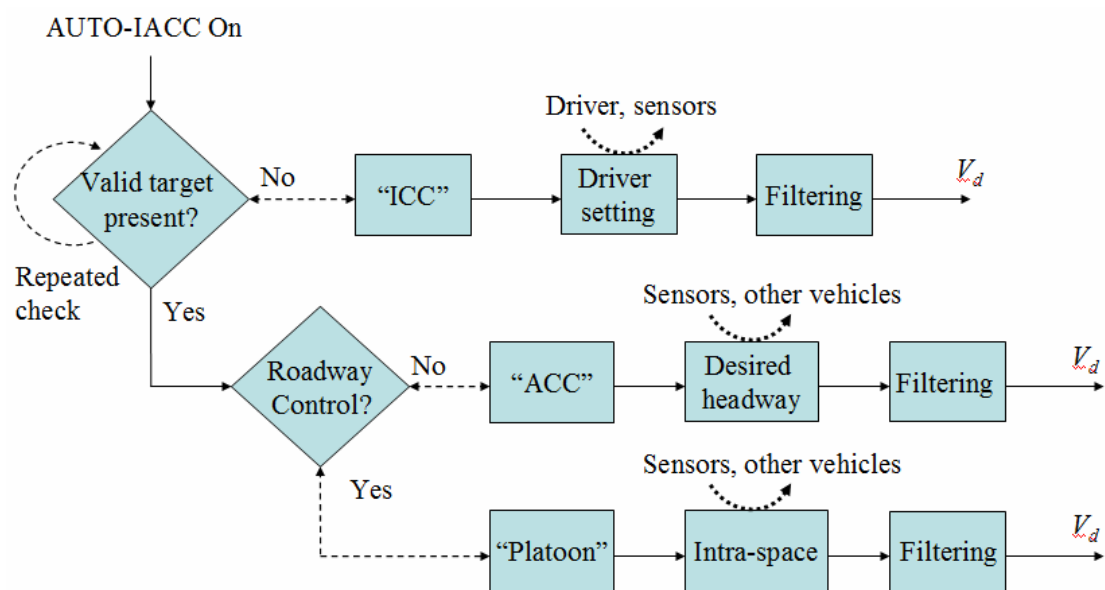
Figure 2-2 Switching logic of difference operation modes

2.2 Hardware design
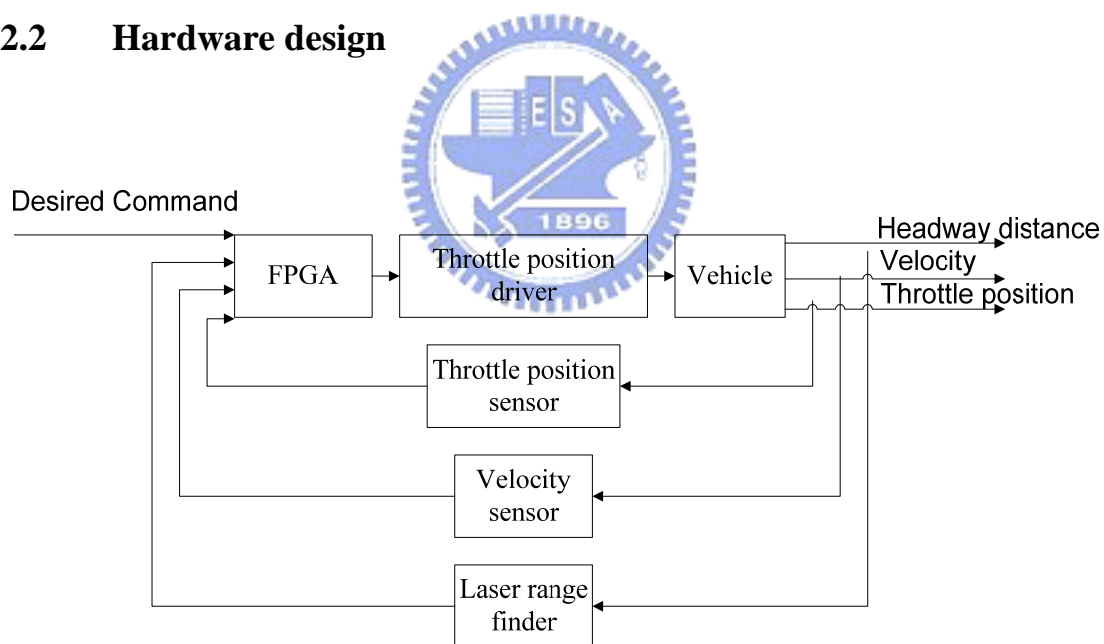
Figure 2-3 Overall structure of experimental system

Figure 2-3 shows the overall structure of the experimental system. The vehicle controller (FPGA) receives real-time vehicle information from the velocity sensor and laser range finder. Furthermore, it computes a desired throttle position for the driver to procure the vehicle control.

2.3   In-vehicle controller design
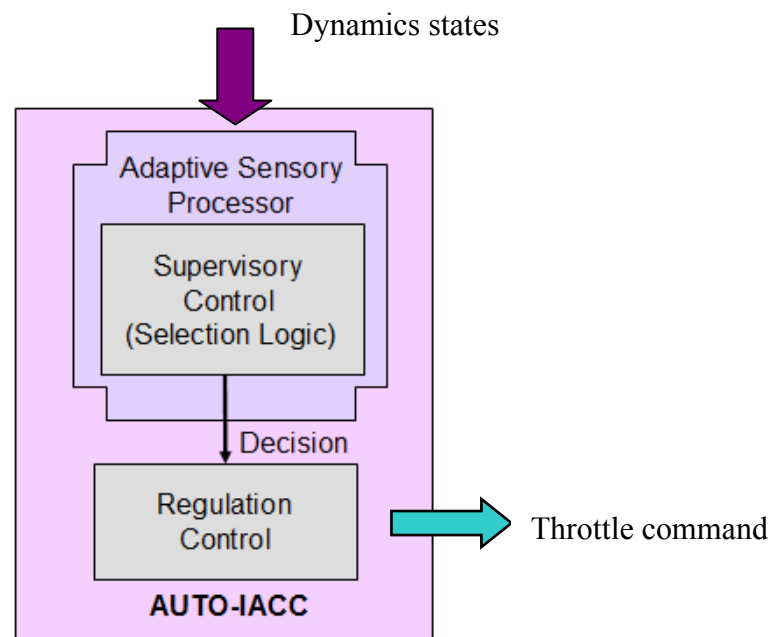
Figure 2-4 Structure of in-vehicle controller design for FPGA board

Figure 2-4 shows the in-vehicle controller that possesses a hierarchical framework including an adaptive sensory, supervisory control and a regulation control.

The adaptive sensory processor passes the supervisory control in-vehicle information first of all. The operation mode of the in-vehicle system is decided by the supervisory control. If the operation mode is ICC, the supervisory control computes a suitable acceleration that the driver can operate a snug vehicle according to the velocity command of the throttle driver. If the operation mode is ACC, the supervisory control computes a safe headway distance and then calculates a safe velocity that the driver can operate a snug vehicle. If the operation mode is platoon, the suitable headway distance is calculated as a fixed value decided by the driver.

Figure 2-5 shows the structure of the supervisor control. The supervisory control finally forwards a safe velocity command to the regulation control in any mode.

According to the safe velocity command, the main job of the regulation control is to drive the throttle pedal. It makes the velocity of the following vehicle reach the required velocity.

- Current velocity of vehicle
- Measured distance

- Desired velocity (ICC)
- Headway time (ACC)
- Intra-spacing (Platoon)

Stage I

Desired acceleration

$$(i)\,|a_f + (r - r_{des})| < a_{f\max}$$
$$a_{fdes} = \frac{1}{\sigma}(KS + \dot{r})$$
$$(ii)\,|a_f + (r - r_{des})| > a_{f\max}$$
$$a_{fdes} = \frac{\dot{a}_f}{K} \pm a_{f\max}$$

Desired acceleration

Stage II

Desired velocity

$$v_f = \min\{v_{f\_ICC}, v_{f\_ACC\,or\,Platoon}\}$$
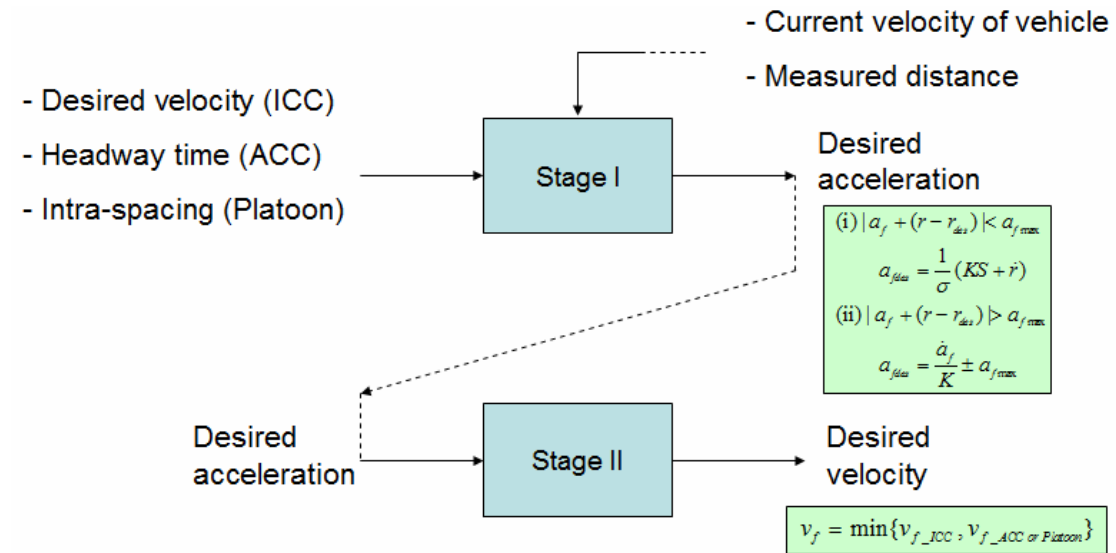
Figure 2-5 Structure of supervisory control

Fuzzy Logic for Throttle

v_d e_v $\int$ K_{IB} K_{PB} e_{vt}

Throttle driving signal
$(u_{throttle})$

v $\dfrac{d}{dt}$ K_{DB}
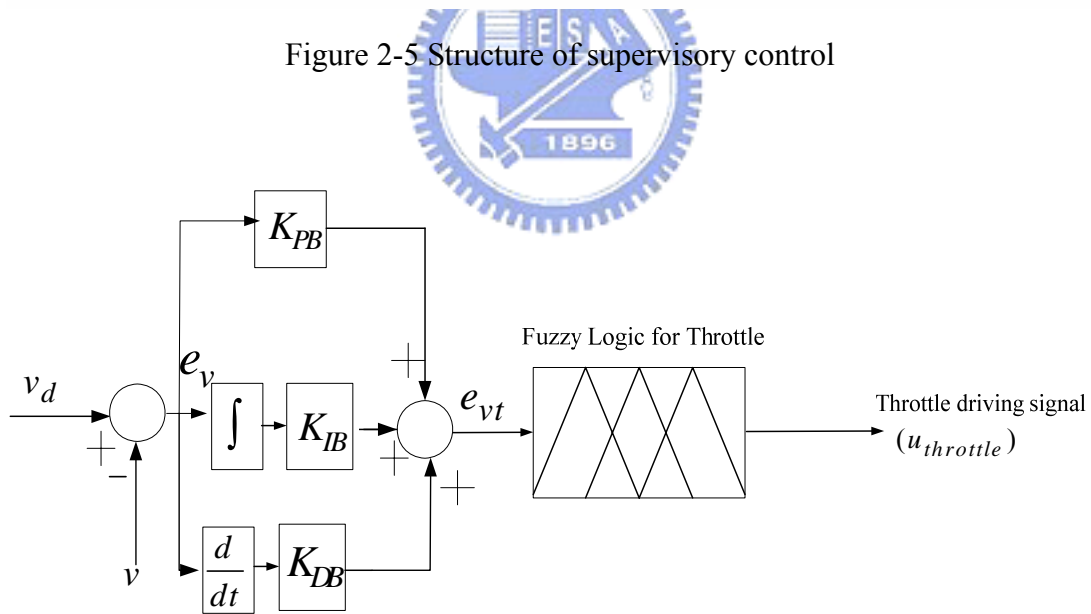
Figure 2-6 Structure block diagram of regulation control

Fuzzy logic control (FLC) is used to control as show in Figure 2-6. Because a design of the transmission system is a complex problem, to achieve an exact velocity control is hard by the traditional control. Besides, the FLC is the optimum design

13

leading a hierarchical framework in because it surmounts the most choke point by the

other control methods. It makes the system reach the smooth purpose on low speed or

changing the gear.

Chapter 3　　Peripheral Interface

The platform of experimental system is SAVRIN 2400 c.c. as show in Figures 3-1 and 3-2. Table 3-1 shows the sample specification of the plant.

Table 3-1 Specification of the plant

Mitsubishi Savrin 2.4	
Engine type	L4 DOHC 16V VVT+DMM
Exhaust	2400 cc
Horsepower (hp/rpm)	150/6250
Torsion　(kgm/rpm)	19.2/3000
Transmission	INVECS-II SPORTS-MODE 4 A/T
Weight	1640 kg

Besides, the vehicle was refitted in the light of demands that included a velocity sensor, throttle position sensor, range finder and a DC motor for driving throttle position. Moreover, development tools were joined for a tachograph (MicroAutoBox) and an in-vehicle controller (FPGA). Figure 3-3 shows the relation of overall elements.

Figure 3-1 Front view of the plant
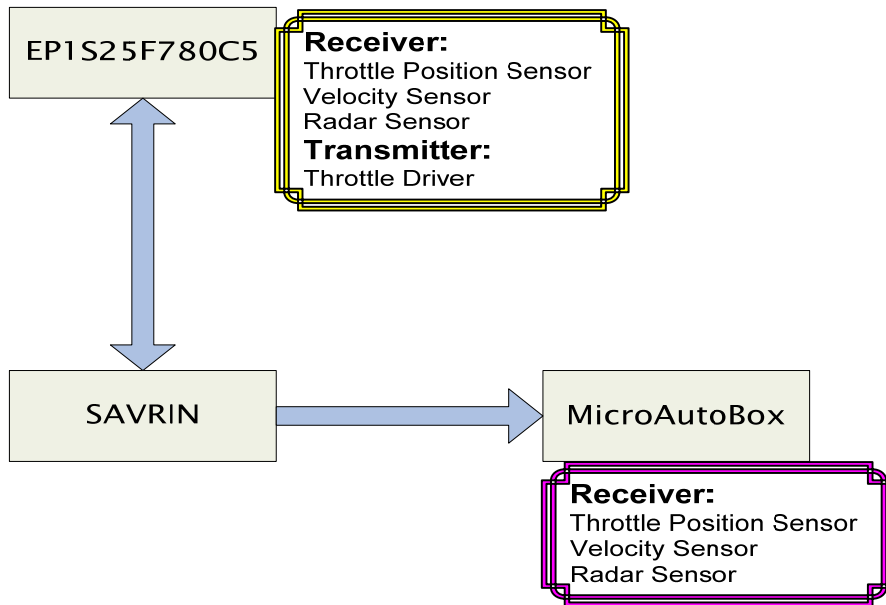

Figure 3-2 Lateral view of the plant

Figure 3-3 Hardware structure of the in-vehicle system
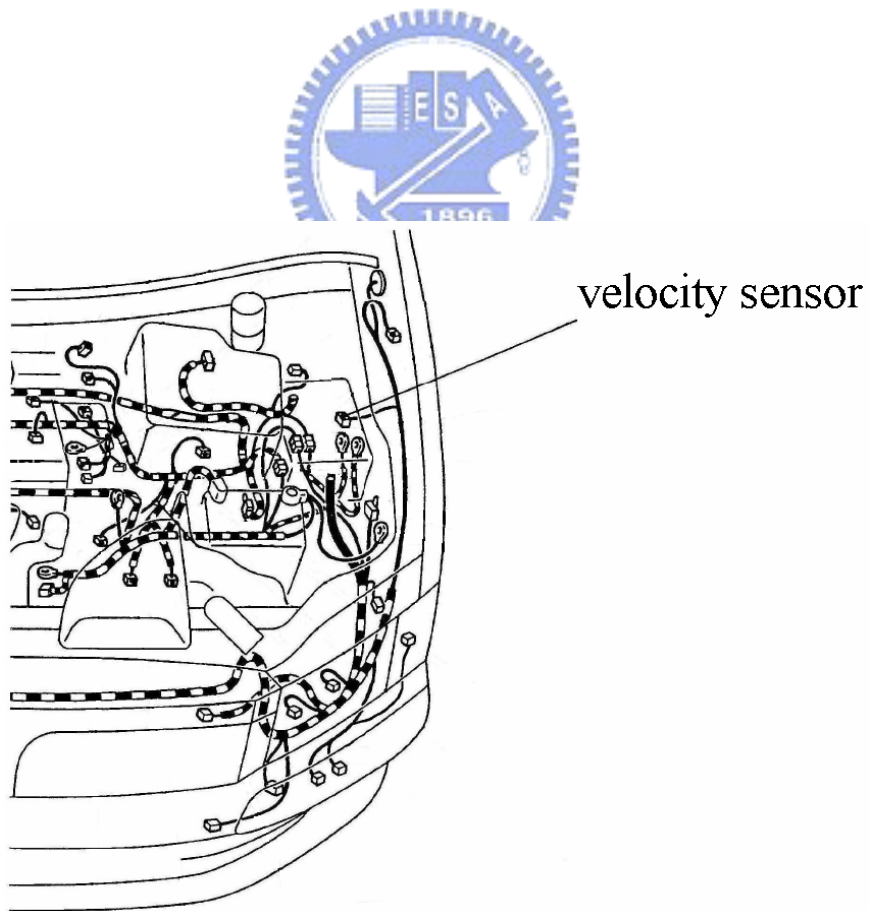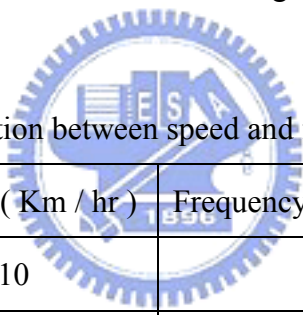
Figure 3-4 Location of the velocity sensor

3.1   Velocity sensor

In the in-vehicle system, one of the most important feedback information is the real-time velocity. Therefore it is a very important task to decode the velocity from the velocity sensor. In Figure 3-4, it shows where we draw out the speed signal. The velocity and its frequency are measured practically and listed in Table 3-2. It indicates that the relation between the velocity and its frequency is almost linear. On the assumption of the linear relation, the velocity could be inferred from the velocity signal. Besides the velocity from the velocity sensor is between 12V and 13 V, to turn the voltage signal to 5V has to do. In order to convert the voltage of the velocity signal, a chip named 7805 is used to arrive at the target.

Table 3-2 Relation between speed and frequency signal

Velocity (Km / hr)	Frequency of signal (Hz)
10	7
20	14
30	21
40	28
50	35
60	42
70	49
80	56
90	63

Duty cycle: 50

A pulse signal of 2M Hz is used to count when the velocity signal state is high in a period as show in Figure 3-5. And then we can obtain the velocity as:

$$T \doteq \left(\frac{1}{2 \cdot 10^6}\right) 2x = \frac{x}{10^6}$$

$$V = \frac{10}{7} \cdot f = \frac{10}{7} \cdot \frac{1}{T} = \frac{10^7}{7x}$$

Where x is the count of a period, T is the period of the velocity signal, f is the frequency and V is the velocity.
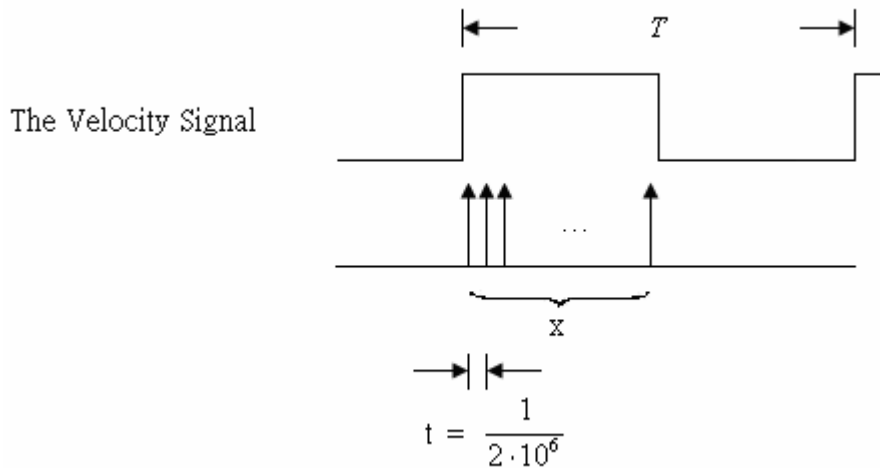
Figure 3-5 A period of the velocity signal

3.2   Throttle position sensor

The other real-time feedback information of the system is the throttle position. Figure 3-6 shows the location of the throttle position sensor. The throttle position is displayed with analog voltage from 0V to 5V. When the vehicle is in static state, the throttle position voltage is about 0.6V. As the throttle is opened more, the throttle position voltage will be increased. It means the more air-gasoline into the engine and more force applies on the vehicle. Thus if we want to exploit the relation, we will

need an instrument to change analog signal to digital signal.
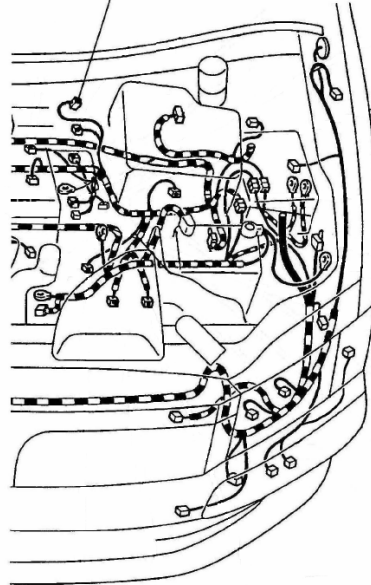
Figure 3-6 Location of the throttle position sensor
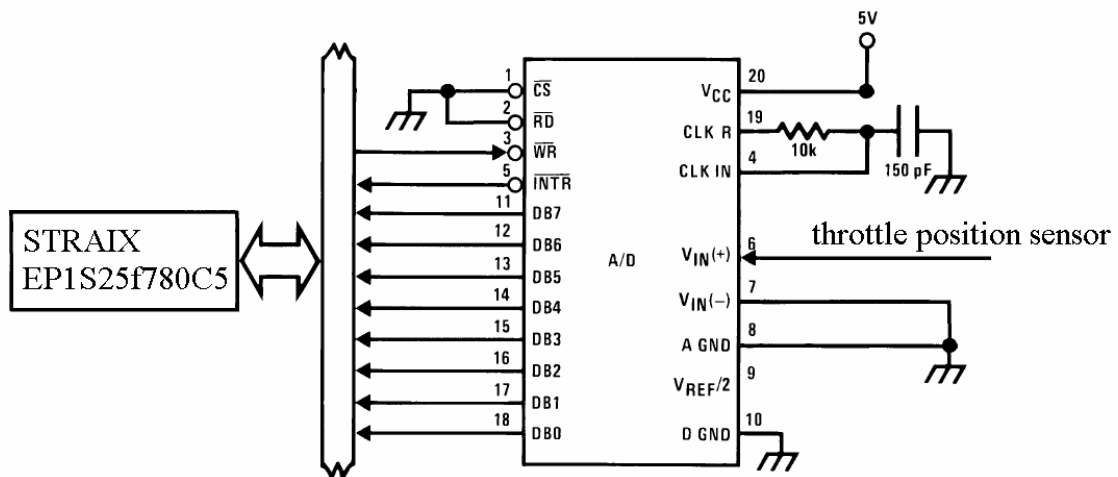
Figure 3-7 Connection between FPGA and ADC0804

An A/D converter called ADC0804 is encoding any smaller analog voltage span to the full 8 bits of resolution shown in Figure 3-7. The reasons we use are its conversion time equal to 100us, easy interface to most microprocessors, TTL

compatible outputs and 0V to 5V analog voltage input range (single + 5V supply).

3.3   Laser range finder

The laser range finder is the most important sensor in the in-vehicle system. Because the scanning range of the laser range finder is larger than an ultrasonic scanner, sound wave scanner and a light wave scanner, we choose it. In Figure 3-8 shows the appearance of it. The data interface between FPGA and the laser range finder is RS-232. Due to different voltage levels shown in Figure 3-9 between each other, there must be a voltage changed circuit. A chip called HIN232 and shown in Figure 3-10 is able to achieve the requirement.

Figure 3-8 Appearance of the laser range finder

Figure 3-9 Voltage levels of RS-232 and TTL
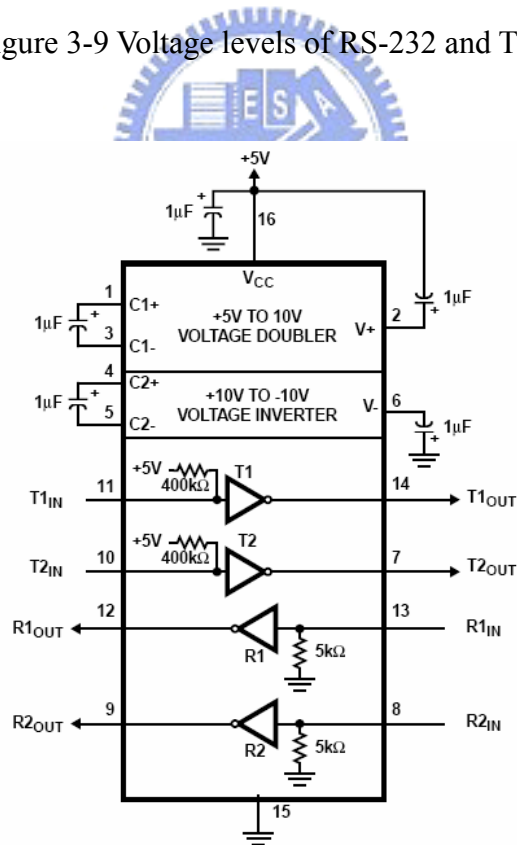
Figure 3-10 HIN232 and operating circuit chart

The shorter period scanner works, the quicker reaction we can act. Therefore,

the operating mode of the laser range finder is configured to reduce scanning period before operating, include changed the baud rate from 9600 to 38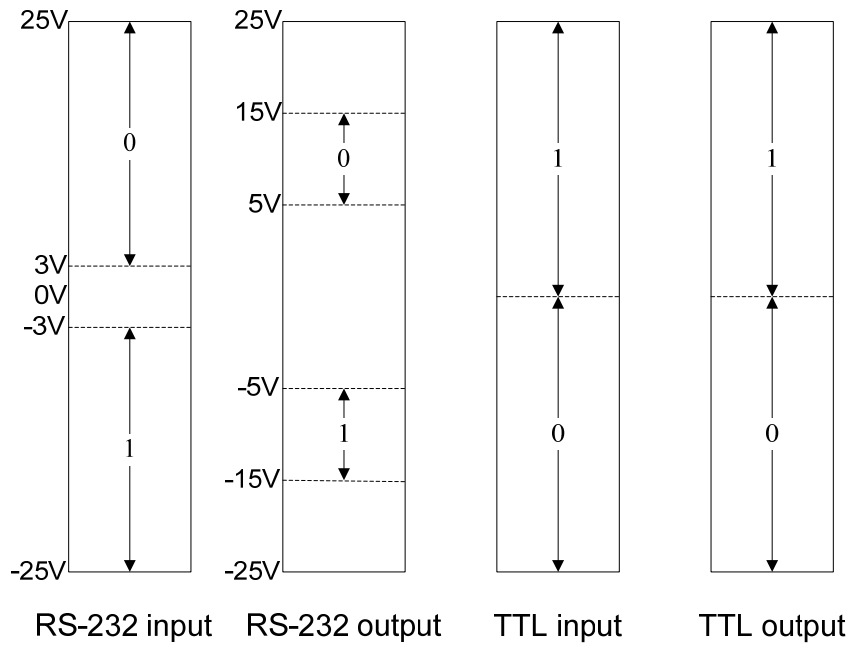400, narrowed the field of view and the angular resolution. After these setup steps are operated, the laser range finder scans once about per 0.13 second as shown in Figure 3-11, which is grabbed from the oscilloscope.
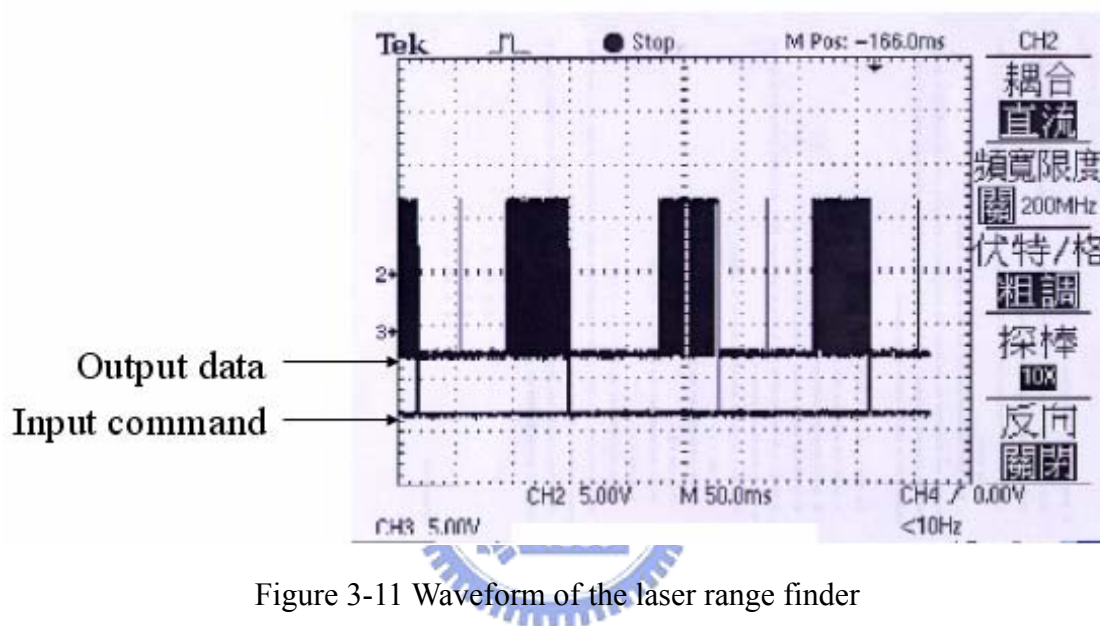
Figure 3-11 Waveform of the laser range finder

If we only grab the distance from the angle 90 degree, the respondent distance may be infinite. It might be the reason of the laser light absorbed by deep color objects, passed through glass without reflection or other reasons. In order to increase the reliability, the distance of angle 88,89,90,91 and 92 degrees are extracted. Then we only deal with the shortest distance among these. There are still chances all of the distances missed even through this step. Therefore we have to think another way. However inaccurate it detect, it is a sensor of the in-vehicle system and the most important mission is to transmit the real-time information to the in-vehicle system true. The supervisory control can deal powerfully with the case.

3.4　　　　Throttle driver interface
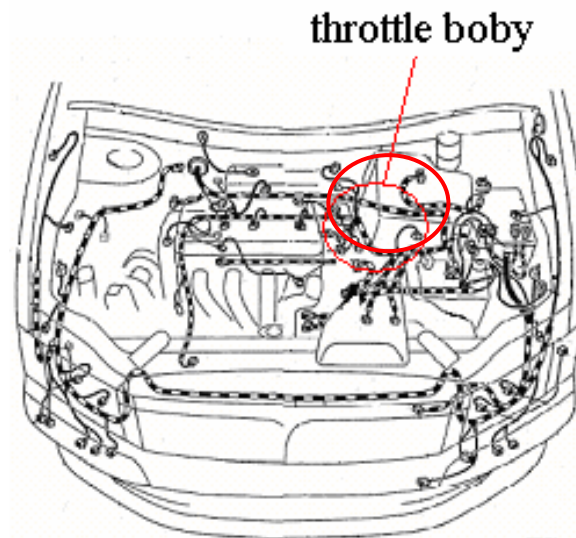
Figure 3-12 Location of the throttle body

　　Here we introduce how to control the throttle pedal. Figure 3-12 shows the location of the throttle body and Figure 3-13 shows the structure of it. The throttle position can adjust the mass of the gasoline and air into the engine. If the throttle was pulled open, the more fuel will be in the engine and the vehicle will run faster in general. If the throttle was set free, the less fuel will be in the engine and the vehicle will slow down. Besides, the throttle is adjusted by a tighter rope. If the pedal pulls tighter than the DC-motor does, the throttle will be controlled by pedal. If the DC-motor pulls tighter more than pedal does, the throttle will be controlled by DC-motor as shown in Figure 3-13. When FPGA controller handles this vehicle, we suppose driver's foot is not on the pedal and throttle is not affected by the driver. Throttle position is fully adjusted by the DC-motor. Therefore, we can control the velocity through adjusting the throttle position indirectly.
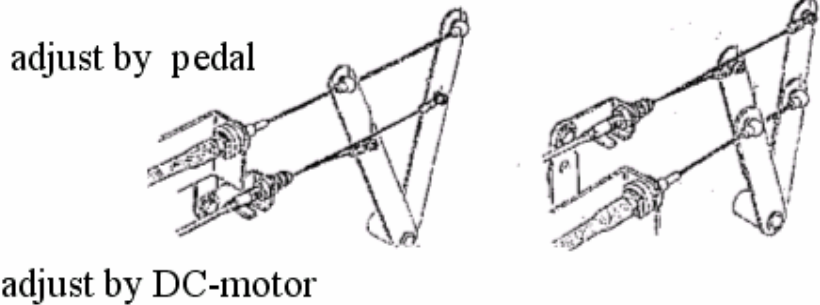
Figure 3-13 Structure of the throttle body
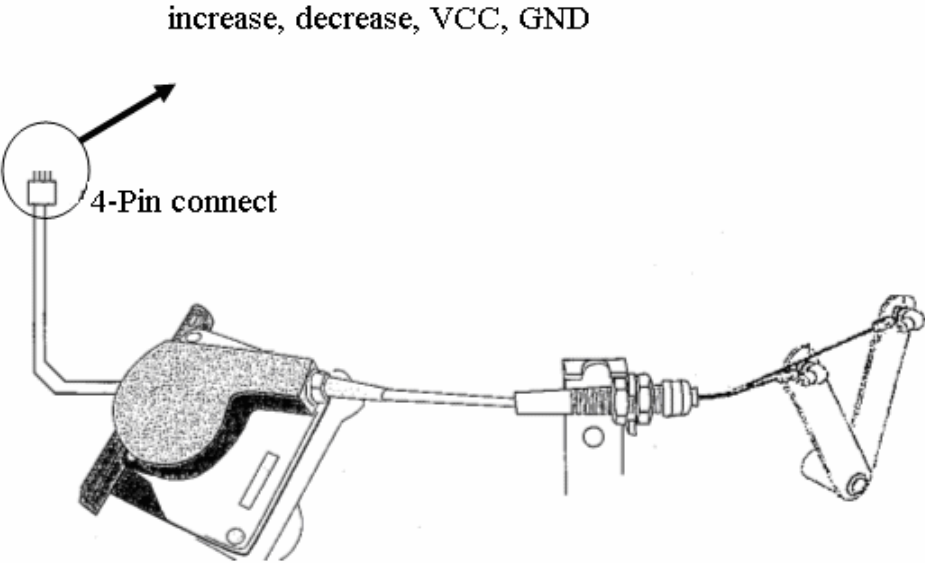
Figure 3-14 Method how DC-motor adjusts the throttle

Next, our problem is to control the throttle position. A DC-motor is used to pull or set free the throttle as Figure 3-14 shows. If the DC-motor pulls the throttle, the position of throttle will be opened and the air- gasoline mixture can flow into the engine. Hence the vehicle will be speeded up. If the DC-motor sets free, the throttle position will be closed and the air- gasoline mixture can not flow into the engine. Hence the vehicle will be slowed down. Finally, we can achieve our goal through the way. We finish our short-distance target to control the velocity.

While the DC-motor is started, it needs almost 0.25A current which can not be

supplied by FPGA itself along. Thus we must have a driver circuit to drive the motor. A chip named TLP250 is used for a DC-DC voltage regulator converter transferring the high voltage signal from FPGA into 12V. There is a digital signal which is 0V or 3V between Pin 2 and Pin 3, and then there will be a digital signal which is 0V or 12V between Pin 7 and Pin 6. Figure 3-15 shows the pin assignment of TLP250.

PIN CONFIGURATION (TOP VIEW)


```
1 : N.C.
2 : ANODE
3 : CATHODE
4 : N.C.
5 : GND
6 : V_O (OUTPUT)
7 : V_O
8 : V_CC
```
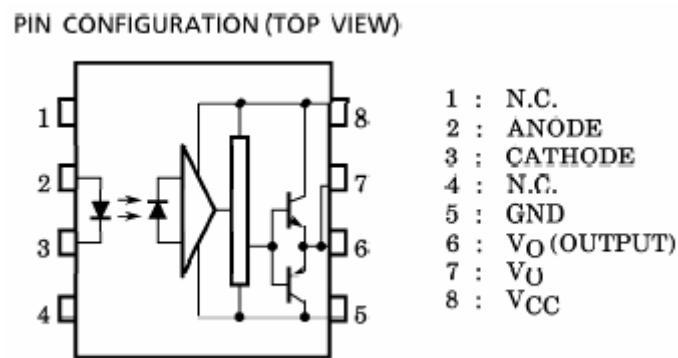
Figure 3-15 Pin assignation of TLP250

We should pay attention to the DC-motor because it is not a typical DC-motor. If there is a constant signal to a DC-motor, typical it will run endless. However, it is not true in our case. In our case, the DC-motor will not move if we arrive the minimum or maximum boundary. The DC-motor will automatically cut off the input current signal at the minimum or maximum boundary. Hence the typical DC-motor driver, H-type circuit is not suitable.

Following the TLP250 is the class B output stage which consists of a complementary pair of transistors (an npn transistor and a pnp transistor) connected in such a way that both cannot conduct simultaneously. It can amplify the current to about 0.3A which can drive the DC-motor. Figure 3-16 shows the layout of the driver circuit. When the signal state is high, the motor is driven. When the signal state is low, the motor is unmoved. Here we don't use the typical PWM signal to drive because the

purpose of the PWM signal is to provide an analog current from 0A to the most for driving. The driver we used like the PWM signal when its duty cycle equal 0% or 100%. And the pnp transistor can receive the current from motor or not when the high transistor state is high.
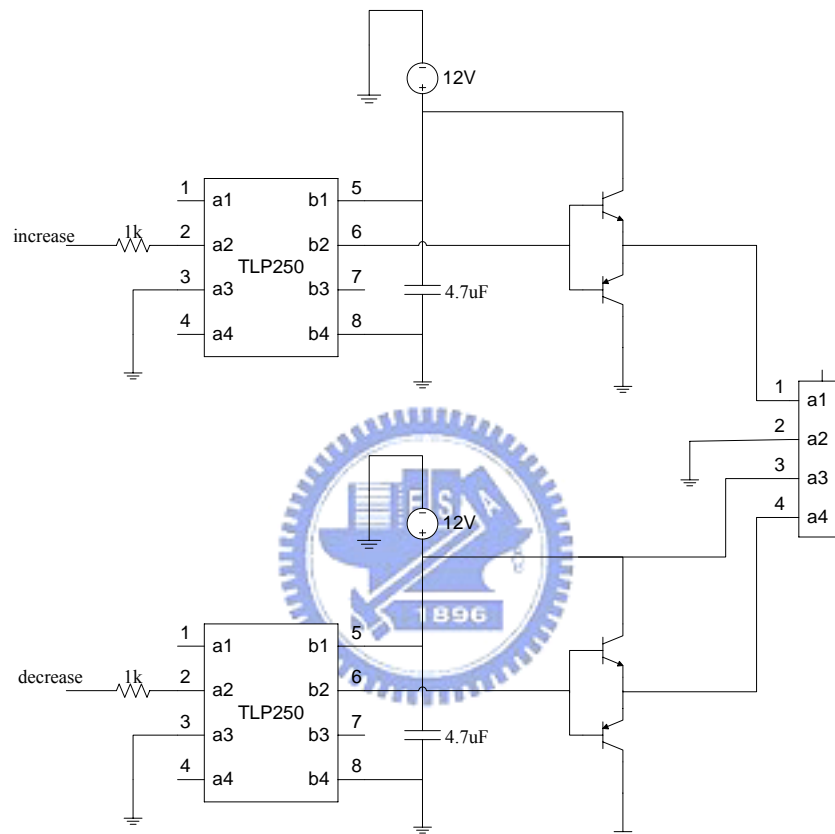
Figure 3-16 Layout of the driver circuit

3.5 Tachograph – MicroAutoBox

Figure 3-17 shows the appearance of the MicroAutoBox from dSPACE. It is a development tool for us to verify the control method easily by the MATLAB function and record the real-time information while going. On the initial stage of developing, it plays a very important role. It is an ideal tool for prototyping, especially in the field of mechanical engineering. It allows the implementation of driving strategies directly

from Matlab/Simulink without requiring the user to write any sort of code or having in-depth knowledge of the electronics involved. According to it, control methods we study could be realized, but relative its price is very high. Because of its price, it must be used for developing. Finally, we must realize the control method on by a low cost FPGA.

Figure 3-17 dSPACE-MicroAutoBox

Figure 3-18 Acquisition system

Figure 3-18 shows the human computer interface. The real-time information will be recorded by the MicroAutoBox with a notebook. By connecting MicroAutoBox, the notebook can display and recode any data we need.

Chapter 4   Autonomy Adaptive Cruise Control Design
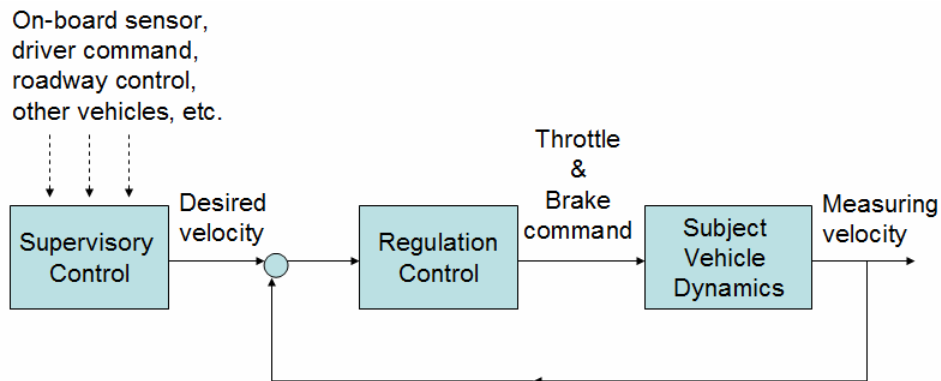
Figure 4-1 Block diagram of the AACC

In this section, the proposed control strategies in the AACC for the ICC, ACC, and platoon control mode are presented. Accordingly in Figure 4-1, the structure of the AACC can be d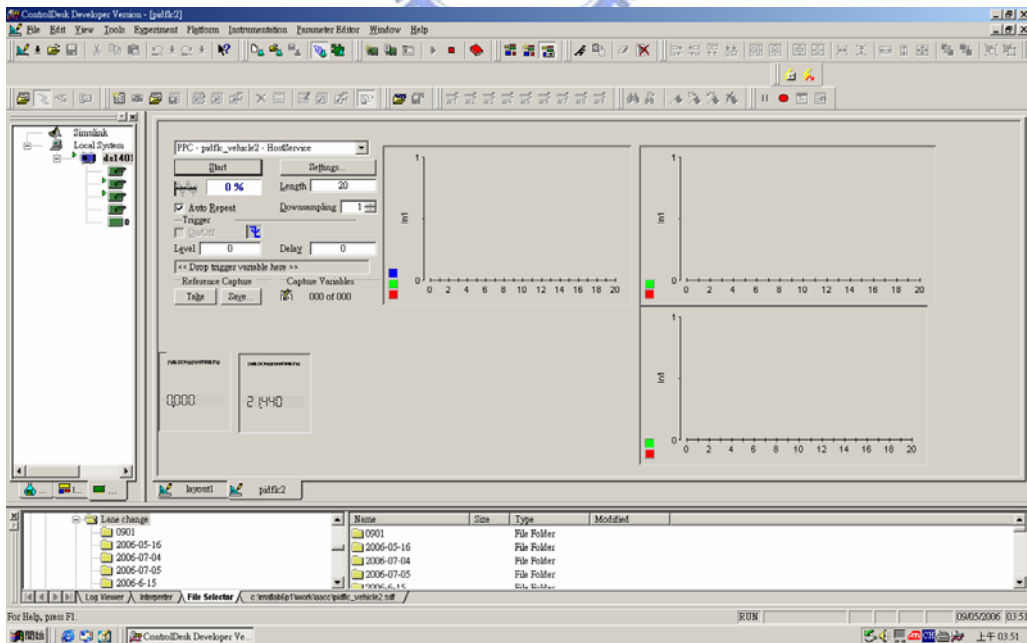ivided into the supervisory control and regulation control, respectively. In addition to calculate a desired velocity based on a commanding velocity or headway distance, the supervisory control also contains the selection logic between different operation modes by recognizing the specifying inputs. Moreover, safety and ride comfort considerations of human factors, are taken into the core of the supervisory control design. The regulation control is responsible to guarantee the subject vehicle to follow the desired velocity command. There are many advantages to this type of control structure. One remarkable reason is that the supervisory control can be designed without much consideration about the regulation control which is developed specifically for the vehicle. The robust supervisory control is essential to be designed such that it can be transferred to another vehicle with only minor

modification.

4.1　　　Regulation control

The objective of the regulation control is to execute the desired velocity commanded from the supervisory control. The vehicle longitudinal dynamics can be described by a set of system composed of various linear and nonlinear subsystems, e.g., engine, automatic transmission in the gear box, brake system, and the rubber tires with respect to roads, etc. Indeed, it is very difficult for control designing based on this complicated model. As to the ill-conditioned and complex model of vehicle longitudinal dynamics, it motivates the employment of fuzzy logic control (FLC) in the regulation control design.
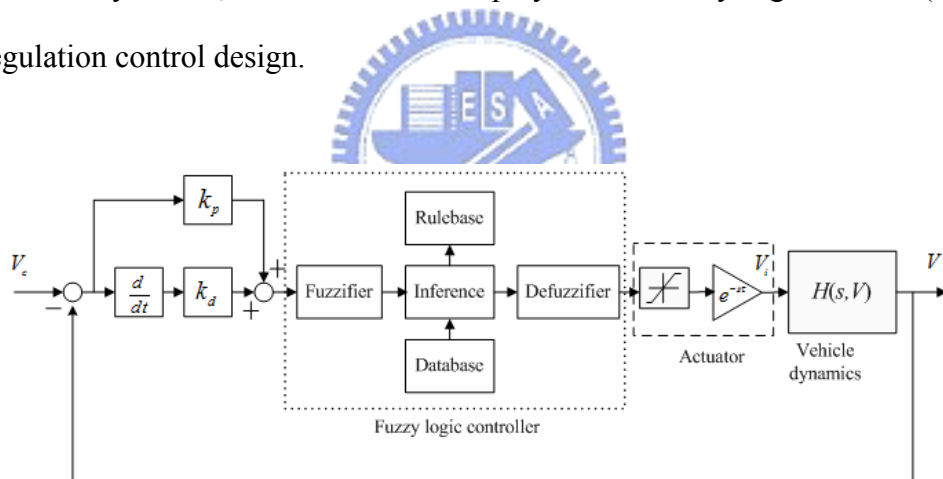
Figure 4-2 The block diagram of the closed-loop control

The block diagram of the regulation control with the vehicle longitudinal dynamics is shown in Figure 4-2. The regulation control scheme is composed of a proportion-derivative (PD) controller and a FLC. There is a single control input defined by the error of the commanded and current velocity, i.e., e $=V_c - V$, and the control output is the applied voltage to the throttle motor actuator. The characteristics of the throttle motor actuator can be modeled as one saturation function with a

31

transport delay. H(s, V) presents the dynamics from the derived throttle angle to the vehicle velocity.

This PD-type FLC with a single-input is convincingly representative to the single-input FLC (SFLC) proposed in [13]. For conventional FLC's, the fuzzy rule base is constructed in a two-dimension (2-D) space for using the error and error change phase-plane, i.e., ($e, \dot{e}$). It can be inspected that most 2-D fuzzy rule bases have the so-called skew-symmetric property. Hence, the switching line which presents the main hyperplane of 2-D fuzzy rule table can be defined as:

$$S : \dot{e} + \alpha e = 0 \qquad (4.1)$$

where α is the slope of the switching line.

Figure 4-3 Derivation of the signed distance

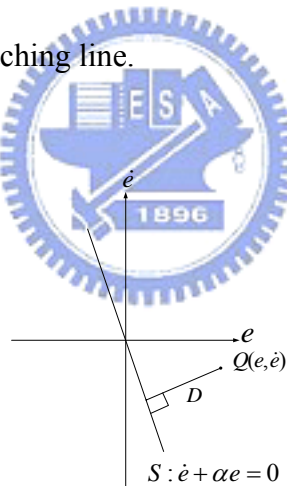The original fuzzy inputs of the error and error change can be replaced by one signed distance, which is defined as the perpendicular distance from an operating point Q($e, \dot{e}$) to the projection point on the switching line S. As illustrated in Figure 4-3, a new fuzzy input of the signed distance can be calculated as

$$D_s = \text{sgn}(s) \cdot D = \text{sgn}(s) \cdot \frac{|\dot{e} + \alpha e|}{\sqrt{1 + \alpha^2}} = \frac{\dot{e} + \alpha e}{\sqrt{1 + \alpha^2}} \qquad (4.\,2)$$

where the sign function is

$$\text{sgn}(s) = \begin{cases} 1 & \text{for } s > 0 \\ -1 & \text{for } s < 0 \end{cases}$$

By viewing (4.1), the equivalent gains of the PD controller in Figure 4-2 can then be obtained from

$$k_d \dot{e} + k_p e = \frac{1}{\sqrt{1 + \alpha^2}} \dot{e} + \frac{\alpha}{\sqrt{1 + \alpha^2}} e \qquad (4.\,3)$$

Now the 2-D fuzzy rule base of the error and error change phase-plane can be reduced into 1-D space of D_s for SFLC as listed in Table 4-1. In Table 4-1, u presents the fuzzy input that it is normalized from D_s. The ranges of the fuzzy input and output are the same from -1 to 1, and the corresponding membership functions are plotted in Figures 4-4 and 4-5, respectively. Control surface of the SFLC is illustrated in Figure 4-6 and it presents the relation between fuzzy input and output.

Table 4-1 Fuzzy rule base of the SFLC

D_s	NB	NS	ZO	PS	PB
u	NBu	NSu	ZOu	PSu	PBu

In the defuzzication operation, the center of mass (COM) method is applied to calculate the control output

$$u^* = \frac{\sum\limits_{i}^{5} \mu_i(D_s) \times u_i}{\sum\limits_{i}^{5} \mu_i(D_s)},$$ (4. 4)

where μ_i represents the weighting value of each rule i, and u_i is the crisp value of each
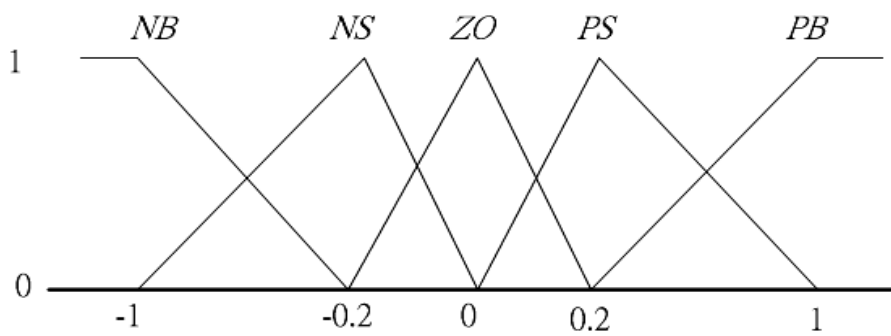
rule consequence.

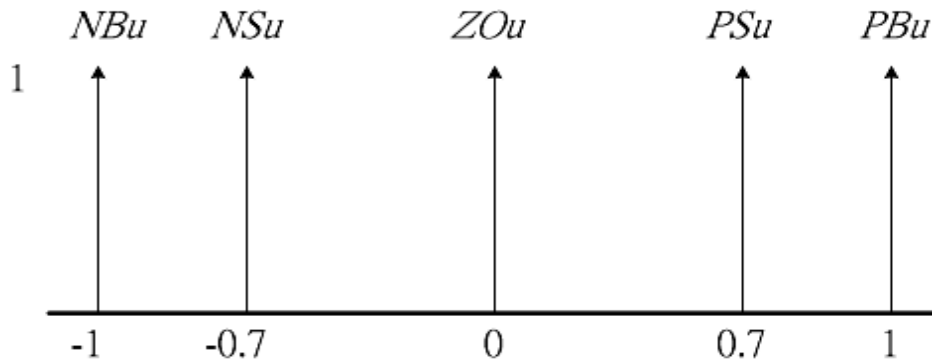Figure 4-4 Membership functions of fuzzy input

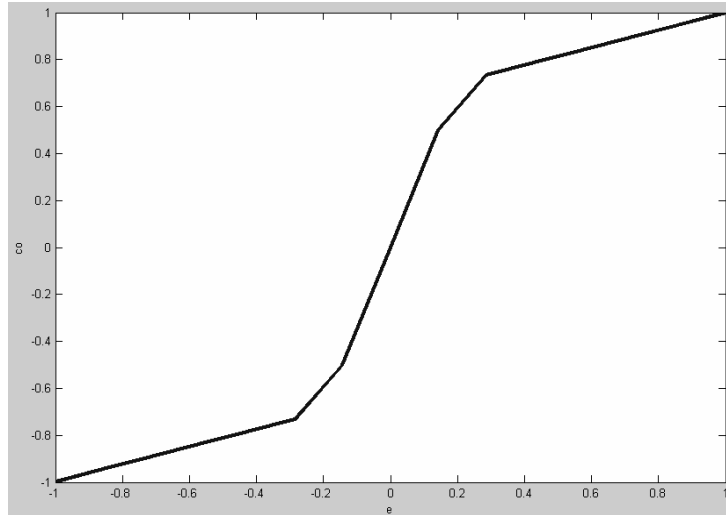Figure 4-5 Membership functions of fuzzy output

Figure 4-6 Control surface of the SFLC

There are many advantages for applying the PD-type SFLC. Regardless of the controlled plant dynamics, it requires only one fuzzy input and a 1-D space of fuzzy rule base. Therefore, the number of tuning parameters in FLC can be greatly reduced. The computation load also can be alleviated for that the number of fuzzy rules is considerably decreased. The parameter k_p and k_d can be calculated beforehand instead of extra computation of the signed distance. Moreover, it is equivalent to the sliding mode control because of a boundary layer such that the closed-loop stability can be achieved. The more detail stability analysis of SFLC can be referred in [13].

The vehicle longitudinal dynamics from the throttle voltage to the vehicle velocity is specified and determined to be a nonlinear function model of varying velocity (e.g., [14, 15]). Based on this model, the stability of the overall fuzzy control system under the effects of system parameters, k_d and k_p, and transport delay τ, can be analyzed by the use of methods of describing function, parameter space and Kharitonov approach. A systematic procedure is presented in our previous work [16] to deal with this problem. Much information of limit cycles caused by the PD-type SFLC can be obtained by this approach, and results show that the limit cycles can be

easily suppressed if the system parameters are chosen appropriately.

4.2   Supervisory control

There are two stages in the supervisory control, as shown in Figure 4-7. In the first stage, the desired acceleration is determined according to the selected operation mode and available feedback signals. In the second stage, the desired acceleration is converted to the desired velocity which is passed into the regulation control.

The supervisory control consists of three operation modes. However, it can be reduced into only two control regimes, velocity tracking and vehicle following, respectively, are needed. The operation modes of ACC and platoon control are governed by the vehicle following control, and the chief difference between the ACC and platoon control mode is the origin of the headway distance.
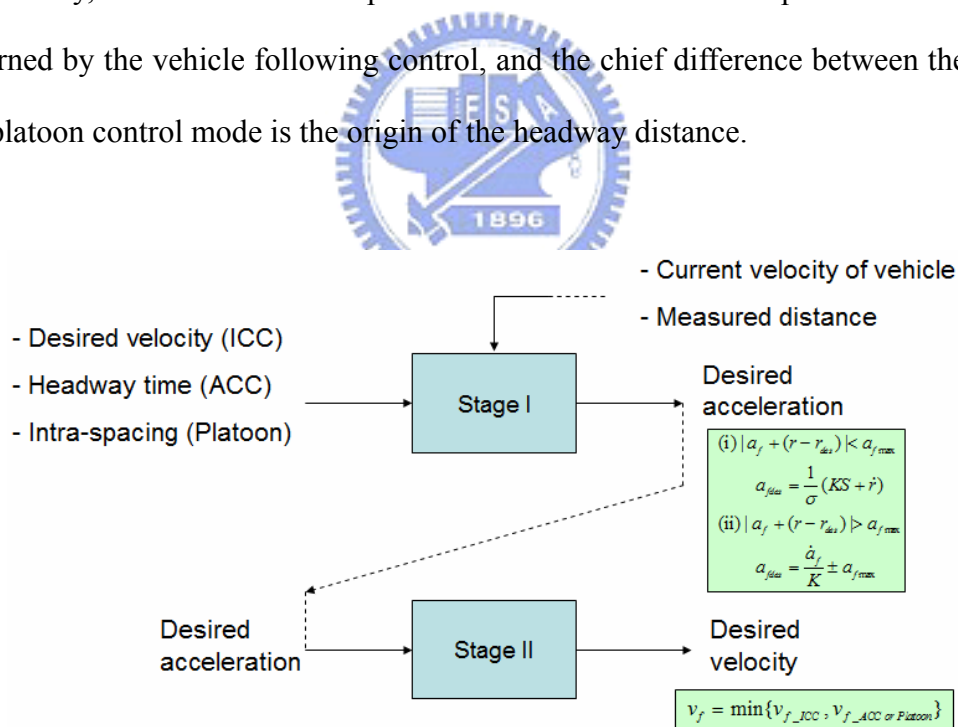

Figure 4-7 Structure of supervisory control

For both control regimes, sliding mode control (SMC) is adopted to design the corresponding control laws. In SMC, one proper surface S in the function of the

system states is required, and the sliding manifold S=0 defined on the closed-loop system is asymptotically stable. To achieve both reachable condition and sliding condition, one must have

$$S\dot{S} < 0, \quad S \neq 0 ,$$ (4. 5)

so that the state trajectory can be forced to the stable manifold in a finite time interval, and then slide toward the equilibrium. With this method of SMC, the control law can be solved through the first derivative of the surface S.

4.2.1 Velocity tracking cruise control design

The objective of the cruise control for velocity tracking is to design the control law of the desired acceleration. Define the velocity error as

$$e_V = V - V_{des}$$ (4. 6)

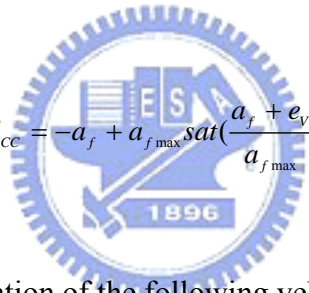and select the sliding surface as

$$S_{CC} = e_V = V - V_{des}$$ (4. 7)

To force $S_{CC} = 0$, the control law can be chosen as

$$\dot{S}_{CC} = -K_{CC} S_{CC}$$ (4. 8)

where $K_{CC} > 0$ is chosen by the designer.

Equation (4. 8) satisfies the global asymptotically stable requirement and also $S_{cc}\dot{S}_{cc} < 0$. Note that the choice of Equation (4. 8) usually includes the discontinuous sign function, e.g., sgn(S), in typical literatures of SMC. However, the chattering phenomena will be caused that also brings some unforeseen noise of high frequency. Thus, the continuous function in Equation (4. 8) is feasible to be implemented for its simplicity.

By differentiating Equation (4. 7), the desired acceleration will be easily solved with Equation (4. 8). To achieve the requirement of ride comfort, it should keep the acceleration command bounded to the desired one a_{fmax} especially while the initial value of e_V is large. Therefore, the sliding surface in Equation (4. 7) can be modified into

$$S_{CC} = -a_f + a_{f\max} sat(\frac{a_f + e_V}{a_{f\max}})$$ (4. 9)

where a_f is the current acceleration of the following vehicle, and

$$sat(x) = \begin{cases} x, & as\ |x| < 1 \\ sign(x), & as\ |x| \geq 1 \end{cases}$$

For the case of $|a_f + e_V| < a_{f\max}$, the sliding surface of Equation (4. 8) is identical to the one of Equation (4. 7). The desired acceleration can be solved as

$$a_{f_{des}} = \dot{V}_{des} - K_{CC}(V - V_{des})$$ (4. 10)

While $|a_f + e_V| \geq a_{f\max}$, the sliding surface becomes

$$S_{CC} = -a_f \pm a_{f\max}$$ (4. 11)

and the desired acceleration is

$$a_{f_{des}} = \frac{-\dot{a}_f}{K_{CC}} \pm a_{f\,max} \tag{4. 12}$$

Note that the jerk in Equation (4. 12) can be neglected for the intention of constraint in the desired acceleration, i.e., $a_{f_{des}} = \pm a_{f\,max}$.

The control laws in Equations (4. 10) and (4. 12) are rather simple. Since only the velocity of the subject vehicle is required for the velocity tracking mode, implementation of this design is easy and still associated with the consideration of ride comfort.

4.2.2 Velocity following control design

The objective of the vehicle following control for headway distance tracking is to design the control law of the desired acceleration. The control design of vehicle following is used in both ACC and platoon control mode. To begin with the development of a sliding surface, the vehicle following dynamics in terms of using the relative distance R are presented as

$$R = X_p - X \tag{4. 13}$$

$$\dot{R} = V_p - V \tag{4. 14}$$

where X and V are the subject vehicle position and velocity, and X_p and V_p are the preceding vehicle position and velocity.

By employing the headway time strategy, the desired following distance law according to the velocity of the subject vehicle can be obtained by

$$R_{des} = \sigma V + L \qquad (4.\ 15)$$

$$\dot{R}_{des} = \sigma a \qquad (4.\ 16)$$

where σ is regarded as the desired headway time, and L can be viewed as a minimum safety distance or typically a vehicle's length.

The error between the desired and relative headway distance is defined as

$$e_R = R - R_{des} \qquad (4.\ 17)$$

Consequently, two sliding surfaces are investigated in the following by the task of with or without v-v communication.

With the consideration of bounded velocity variation, the sliding surface composed of the error and error variation can be defined as

$$S_{VF} = -a_f + a_{f\max} sat(\frac{a_f + \dot{e}_R + \lambda e_R}{a_{f\max}}) \qquad (4.\ 18)$$

where λ >0 is the sliding surface gain.

For the case of $|a_f + \dot{e}_R + \lambda e_R| < a_{f\max}$, the sliding surface becomes

$$S_{VF} = \dot{e}_R + \lambda e_R = \dot{R} - \dot{R}_{des} + \lambda(R - R_{des}) \qquad (4.\ 19)$$

It is clear to examine that the stability for the sliding surface in Equation (4. 19)

by setting $S_{VF}=0$. The error dynamics $e_R(t)=e^{-\lambda t}$ is asymptotically stable for all positive λ.

By differentiating Equation (4. 19), one obtains

$$\dot{S}_{VF} = \ddot{R} - \ddot{R}_{des} + \lambda(\dot{R} - \dot{R}_{des}) \tag{4.20}$$

To guarantee the reachable condition and asymptotically stability, the control law is chosen the same to Equation (4. 8), namely

$$\dot{S}_{VF} = -K_{VF}S_{VF} \tag{4.21}$$

where $K_{VF}>0$ is chosen by the designer.

By virtue of Equations (4. 20) and (4. 21), the desired acceleration can be solved as,

$$a_{f_{des}} = \frac{1}{1+\lambda\sigma}(K_{VF}S_{VF} + a_P + \lambda\dot{R} - \sigma\dot{a}_f) \tag{4.22}$$

While $|a_f + \dot{e}_R + \lambda e_R| \ge a_{f\max}$, the sliding surface becomes

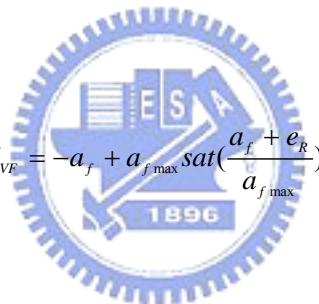$$S_{VF} = -a_f \pm a_{f\max} \tag{4.23}$$

and the desired acceleration is

$$a_{f_{des}} = \frac{-\dot{a}_f}{K_{CC}} \pm a_{f\max} \tag{4.24}$$

Note that the jerk of the following vehicle in Equation (4. 24) can be neglected

the same for the intention of constraint, i.e., $a_{f_{des}} = \pm a_{f\max}$. Interestingly, the acceleration of the following vehicle is primarily used in the sliding surface yet erased in the final control form.

Equation (4. 22) reveals that the acceleration of the preceding vehicle and the jerk of the following vehicle are required. However, these data are difficult to measure in implementation directly. Although the knowledge of the preceding vehicle can be obtained by v-v communication, it can not be supposed that all other vehicles have the communication device. Besides, the jerk even could be estimated by numerical methods, but the computation cost will increase.

To overcome the disadvantage in Equation (4. 22), the sliding surface can be modified as

$$S_{VF} = -a_f + a_{f\max} sat(\frac{a_f + e_R}{a_{f\max}}) \qquad (4.\ 25)$$

For the case of $|a_f + e_R| < a_{f\max}$, this sliding surface is obviously stable since S_{VF} =0 as e_R =0. By choosing the same control law as Equation (4. 21), the desired acceleration can be derived as

$$a_{f_{des}} = \frac{1}{\sigma}(K_{VF} S_{VF} + \dot{R}) \qquad (4.\ 26)$$

The result in the case of $|a_f + e_R| > a_{f\max}$ is the same to Equation (4. 24) and the constraint $a_{f_{des}} = \pm a_{f\max}$ is used instead.

In Equation (4. 26), only the rate of headway distance is required. However, one can well imagine that the better performance will be achieved for Equation (4. 22),

since the additional knowledge can improve controlling response of the following vehicle to the behavior of the preceding vehicle.

In the second stage, the conversion from the desired acceleration to the velocity is designed as

$$\dot{V}_{des} = a_{f\,des} - k_t(V - V_{des}) \tag{4.27}$$

where $k_t > 0$ is a damping gain.

The proper choice of k_t can avoid severe responses for the desired velocity against noise involved in the measurement of headway distance and vehicle velocity. To implement the conversion in discrete time, the differential Equation (4. 27) can be approximated by using Euler's method as

$$V_{des}(k+1) = (1 - Tk_t)V_{des}(k) + T(k_t V(k) + a_{des}(k)) \tag{4.28}$$

where T is the sampling period in control process, and the new value V_{des} (k+1) is computed by the past values $V_{des}(k)$, $V(k)$, and $a_{des}(k)$.

In Section 1.2.4, it has been introduced that the selection logic between the ACC and platoon control mode is dependent on the stimulation of the roadway control. This is constructed in the first stage. As to the selection logic between the ICC and ACC (or platoon) mode, this autonomy scheme can be achieved by adopting the min-operation in the second stage, namely,

$$V_f = \min\{V_{des\_ICC}, V_{des\_ACC \ or \ platoon}\} \tag{4.29}$$

43

Once the valid target is detected, the final desired velocity for the subject vehicle will be determined by the vehicle following control, i.e., $V_f = V_{des\_ACC\ or\ platoon}$; otherwise, the subject vehicle will be back to the velocity tracking cruise control, i.e., $V_f = V_{des\_ICC}$. This approach is intuitive but also easy to implementation.

Chapter 5   Implementation Results

5.1   Design flow and verification

In this chapter, we show experimental results verified in Savrin on the west-east expressway. The velocity range is about from 60 km/hr to 90 km/hr.

A device, MicroAutoBox, is used to record the velocity (km/hr), throttle position voltage (v) and the relative distance (meter). Three different experiment results: ICC mode, ACC mode and platoon mode are developed.
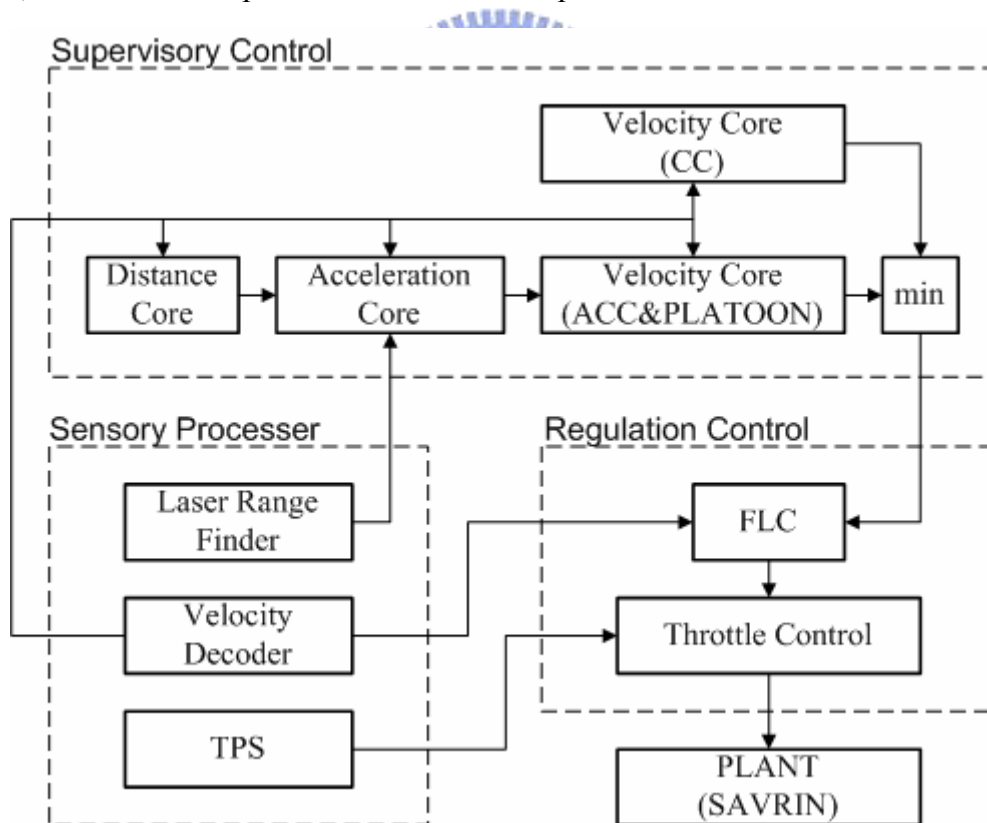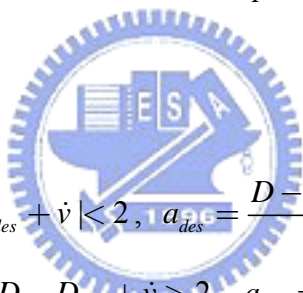

Figure 5-1 Function blocks

Where the distance core decides the desired distance and the operation modes, ACC mode and platoon mode, are selected here.

By reviewing Chapter 3 and Chapter 4, we simplify and verify the control theorem and present function blocks in Figure 5-1. The output signal, the desired distance can be modified as:

$$D_{des} = const \quad \text{or} \quad v \cdot \sigma \tag{5.1}$$

Where D_{des} is the desired distance, v is the real velocity and σ is the headway time defined by the driver. If the operation mode is platoon mode, D_{des} is a constant value presented the headway distance. If the operation mode is ACC mode, it is computed by the real velocity.

In the next place, the acceleration core computes the output signal, the desired acceleration is modified as:

$$\text{If } |D - D_{des} + \dot{v}| < 2, \quad a_{des} = \frac{D - D_{des} + 2\dot{D}}{2\sigma} \tag{5.2}$$

$$\text{If } D - D_{des} + \dot{v} > 2, \quad a_{des} = 2 \tag{5.3}$$

$$\text{If } D - D_{des} + \dot{v} < -2, \quad a_{des} = -2 \tag{5.4}$$

Where a_{des} is the desired acceleration and the threshold limit value is decided to match the acceleration of the vehicle.

At last, the output signal of the velocity core is the desired velocity. The desired velocity of CC mode and ACC mode (or platoon mode) are computed respectively. They are resolved by getting the minimum of them. The output signal of the velocity core is presented as:

$$v_{des} = (a_{des} + k \cdot v)T + (1 - k \cdot T) \cdot v_{des}[n-1] \tag{5.5}$$

and the acceleration of CC mode is modified as:

$$a_{des} = \dot{v}_{des} + 0.75(v_{des} - v),$$ (5.6)

where T is the sampling time , v_{des} is the desired velocity, a_{des} is the desired acceleration and k is the damping parameter. Parameters, T and k, are defined by the driver for the ride comfort and we set T for 0.01sec and k for 1.

Section 5.2 presents the intelligent cruise control. It is the basic of the autonomy adaptive cruise control. After that, ACC and platoon were verified in Section 5.2.1 and 5.2.2.

5.2   Experimental resoults

5.2.1 Curise control

On the west-east expressway, we test the regulation control of CC mode when the desired velocities are 60, 70, 80 and 90 km/h, respectively. The experimental results including the velocity and the throttle position of the vehicle are shown in Figures 5-2, 5-3, 5-4 and 5-5. We can clearly find that the real-time data on the different velocities are matched with the desired commands.
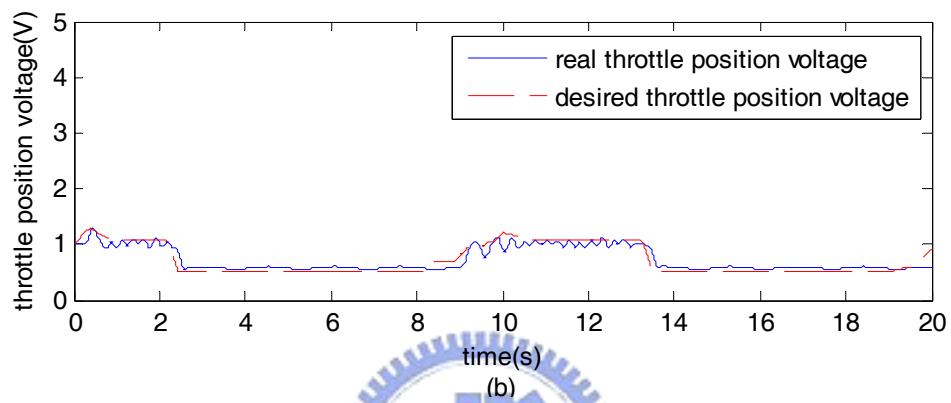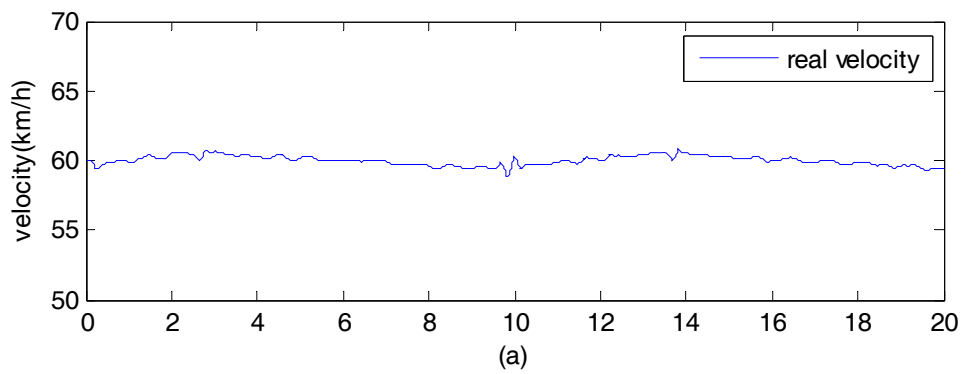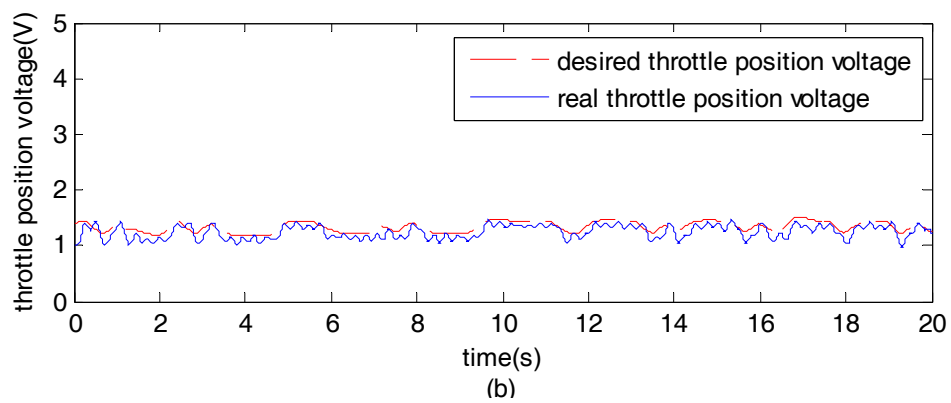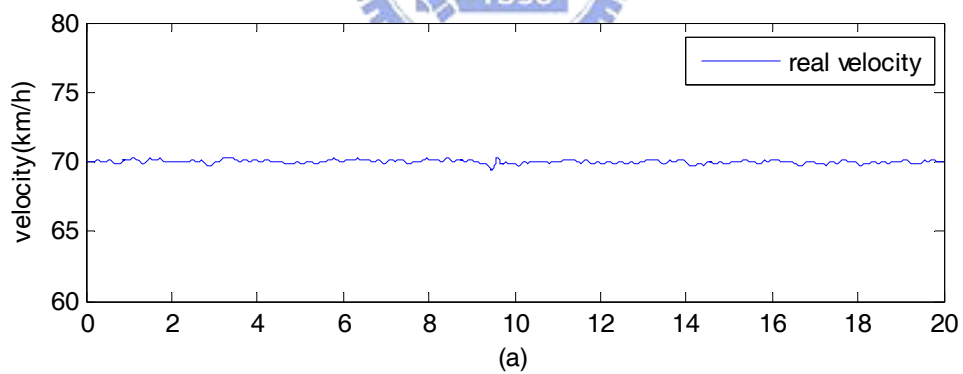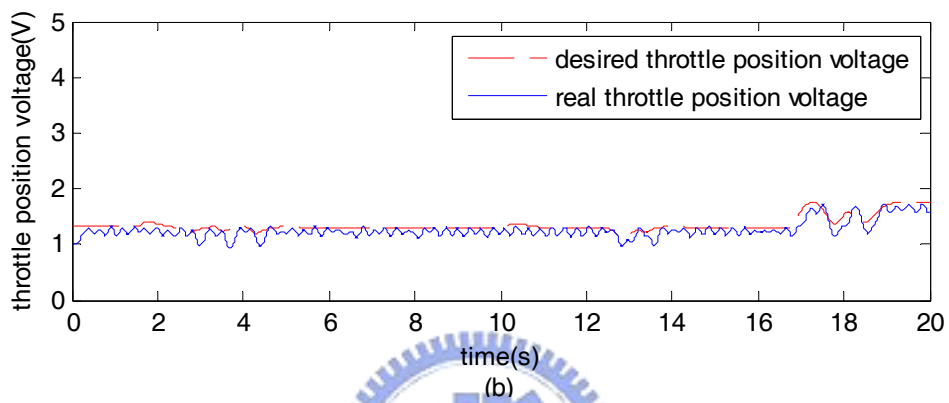
Figure 5-2 CC mode of 60 km/h
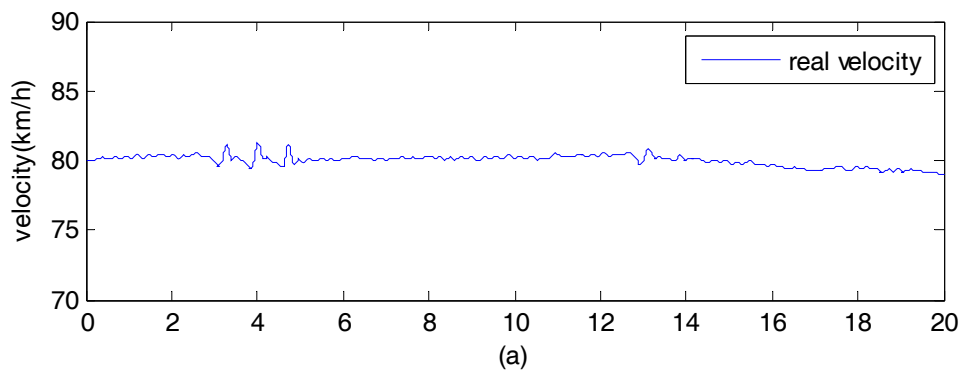

Figure 5-3 CC mode of 70 km/h

Figure 5-4 CC mode of 80 km/h
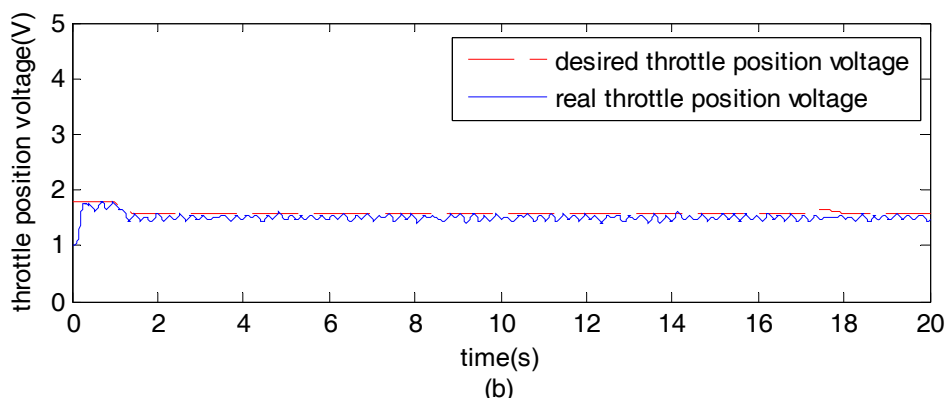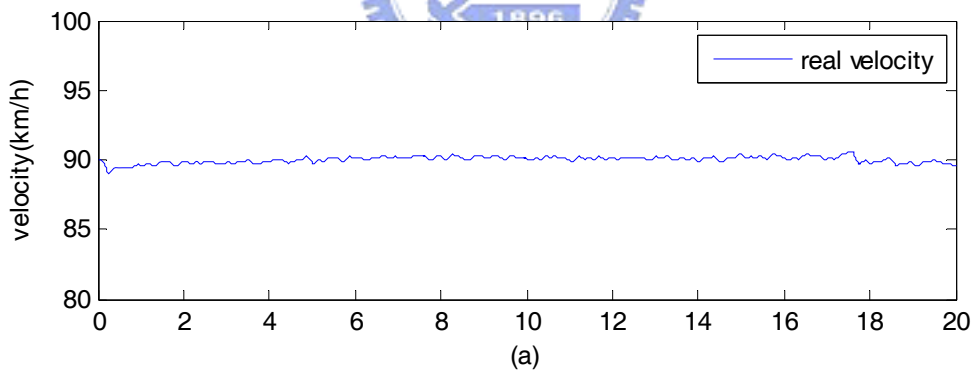
Figure 5-5 CC mode of 90 km/h

Table 5-1 Compare the real velocity in different desired velocities

	Desired velocity (km/h)	$\lvert e_v \rvert_{avg}$ (km/h)	$\lvert e_v \rvert_{avg}$ (%)	$\lvert e_v \rvert_{max}$ (km/h)	$\lvert e_v \rvert_{max}$ (%)
Figure 5-2	60	0.3096	0.52	1.2398	2.01
Figure 5-3	70	0.1453	0.2	1.0464	1.49
Figure 5-4	80	0.3336	0.4	2.0688	2.59
Figure 5-5	90	0.2547	0.28	0.9196	1.02

Table 5-1 shows the performance of the regulation control, where e_v represents the error between the real velocity and the desired velocity, $\lvert e_v \rvert_{avg}$ is the absolute of the mean error and $\lvert e_v \rvert_{max}$ is the absolute of the mean error.

(a)

(b)
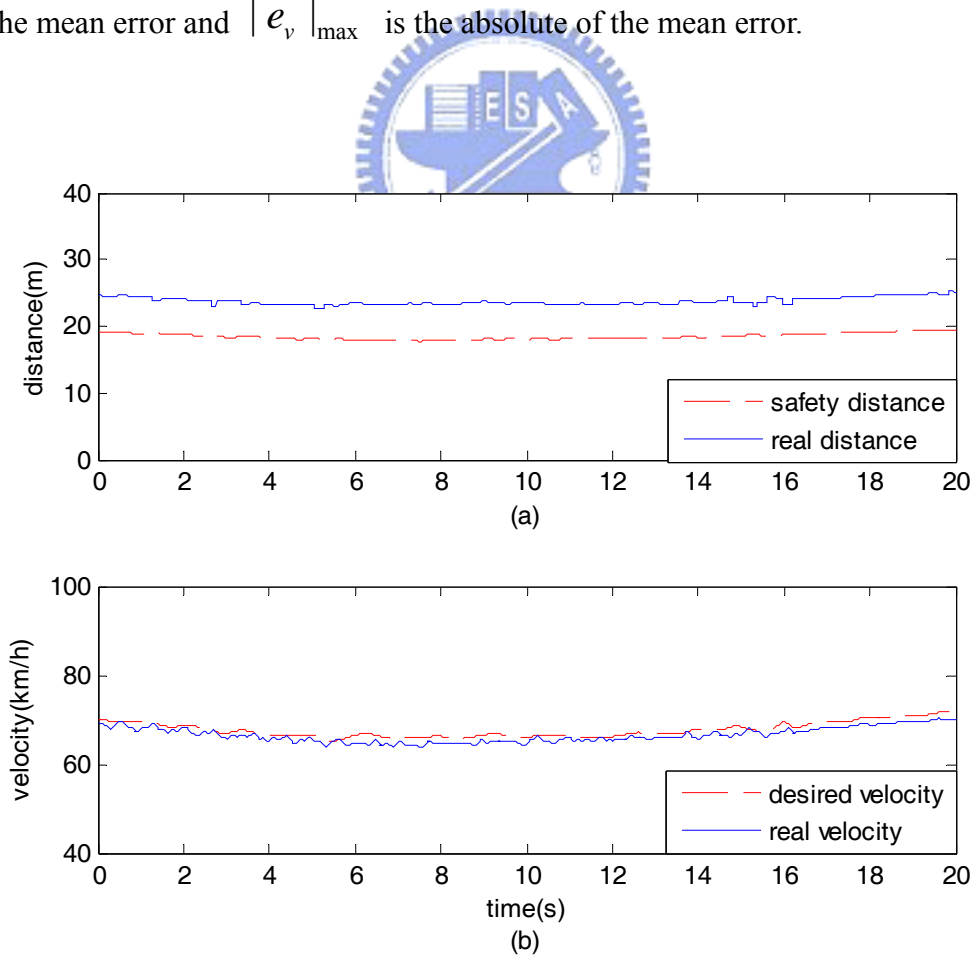
Figure 5-6 ACC mode of supreme 90 km/h
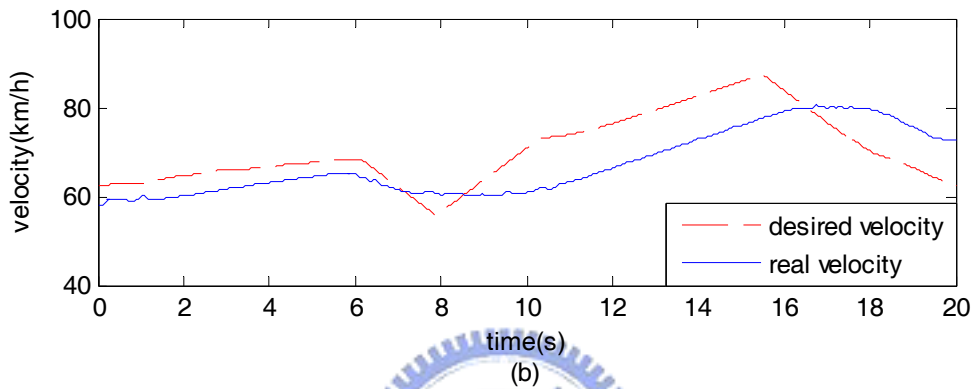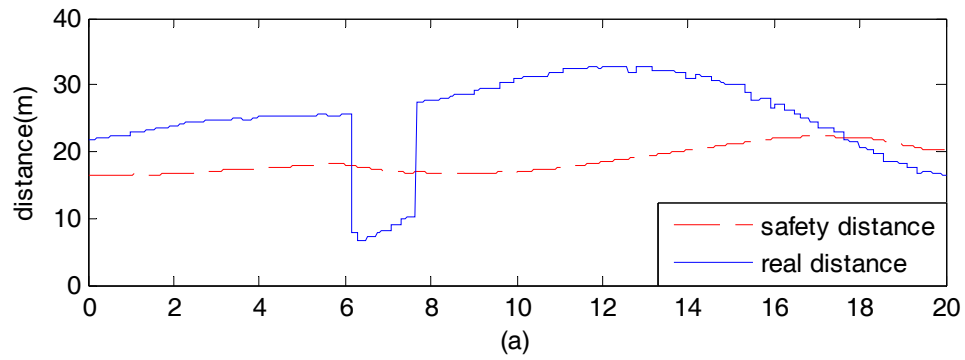
Figure 5-7 ACC mode with a detection error from the laser range finder

5.2.2 Adaptive cruise control

In the following subsections, for the reason of safe driving, the desired distance (D_{des}) is defined as:

$$D_{des} = D_{safety} + 4 \quad \text{(meter)}, \qquad (5.7)$$

where D_{safety} means the safety distance.

In our experimental results, Figure 5-6 (a) and (b) show the time responses of the distance and the velocity of the vehicle, respectively. It is clear that the better performance in ACC mode can be achieved by out approach.

51

The time response in an abominable environments are shown in Figure 5-7 when it has a detection error and the velocity of the target is changing by a large margin. During 0 - 6 seconds, the front car goes with higher speed and the desired velocity increases. During 6 - 8 seconds, the detection error happens because the vehicle meets lowers and upper slopes. The controller should be decelerated for safety. During 8 - 12 seconds, the relative velocity increases because the velocity of the target is changing by a large margin. During 12 - 16 seconds, the relative velocity decreases. During 16 - 20 seconds, the desired velocity reduces because the relative distance is decreased and the acceleration is increased.

In the light of the detection error, the acceleration of the desired velocity is bound to match with the acceleration of the engine brake. In the next place, the real distance is reduced rapidly. In this scene, the desired velocity is also reduced rapidly. In the future, the electrical brake system will be added on the system to get the better performance of car following.
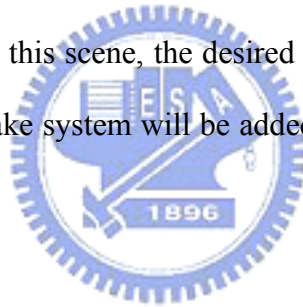
5.2.3 Platoon control
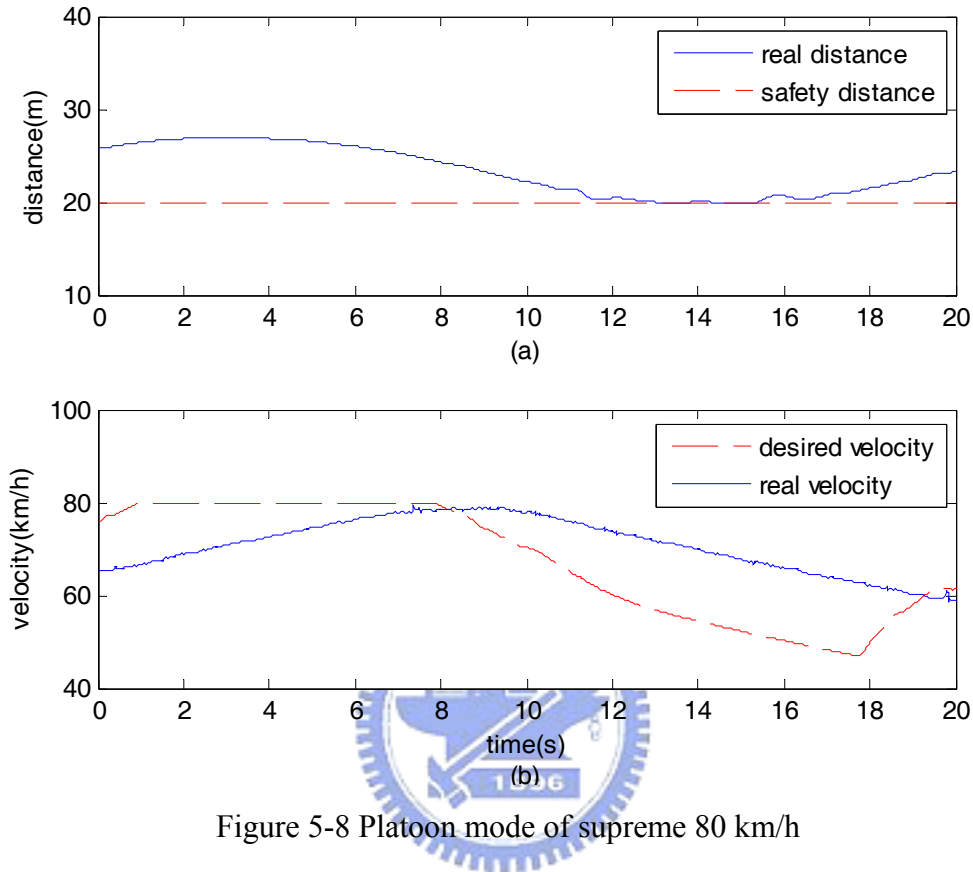
Figure 5-8 Platoon mode of supreme 80 km/h

Figure 5-8 represents the time response of the platoon mode. During 0 - 8 seconds, the front car goes with higher speed. The desired velocity increases and bounds in 80 km/h. During 8 - 18 seconds, the real distance is close to the safety distance in Figure 5-8 (a). By observing Figure 5-8(b), the desired velocity start to decrease when the time is at 8th second.

In ACC mode or platoon mode, we can find that the real distance is difficult to track the desired distance. The most important reason is from the acceleration of the vehicle. The following vehicle has no enough power to track the desired velocity and the reason will be introduced in Section 5.3.2. But the most important function of the system is to keep the safe distance.

Figure 5-9 All circuits

Laser range finder circuit

Velocity signal circuit

DC motor driver

Throttle position
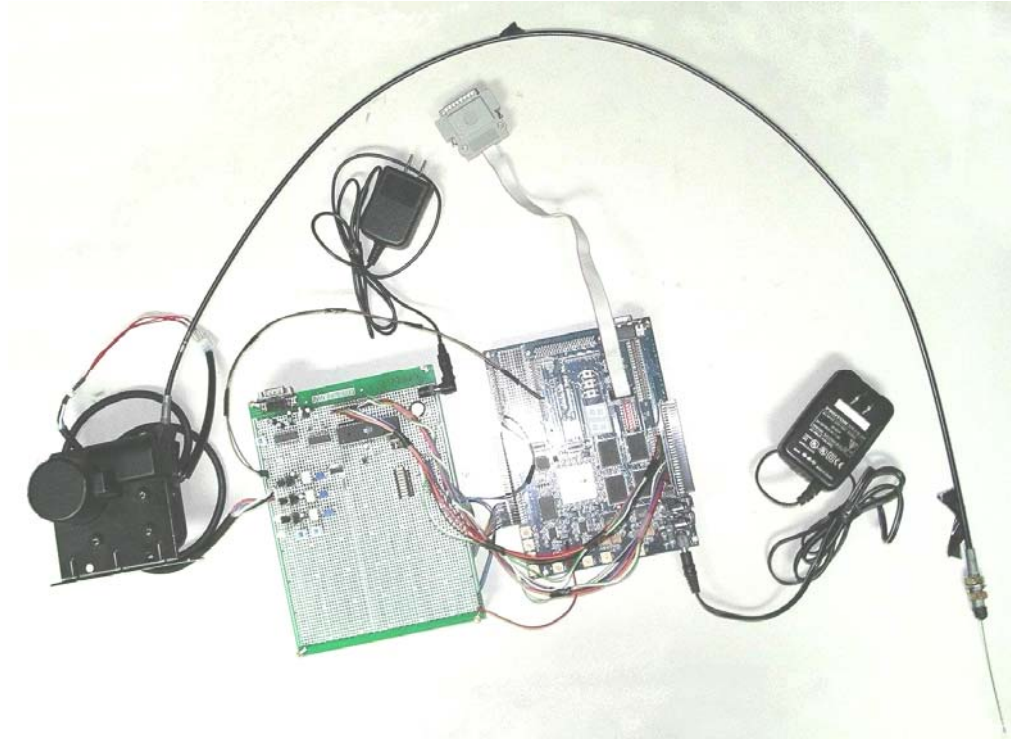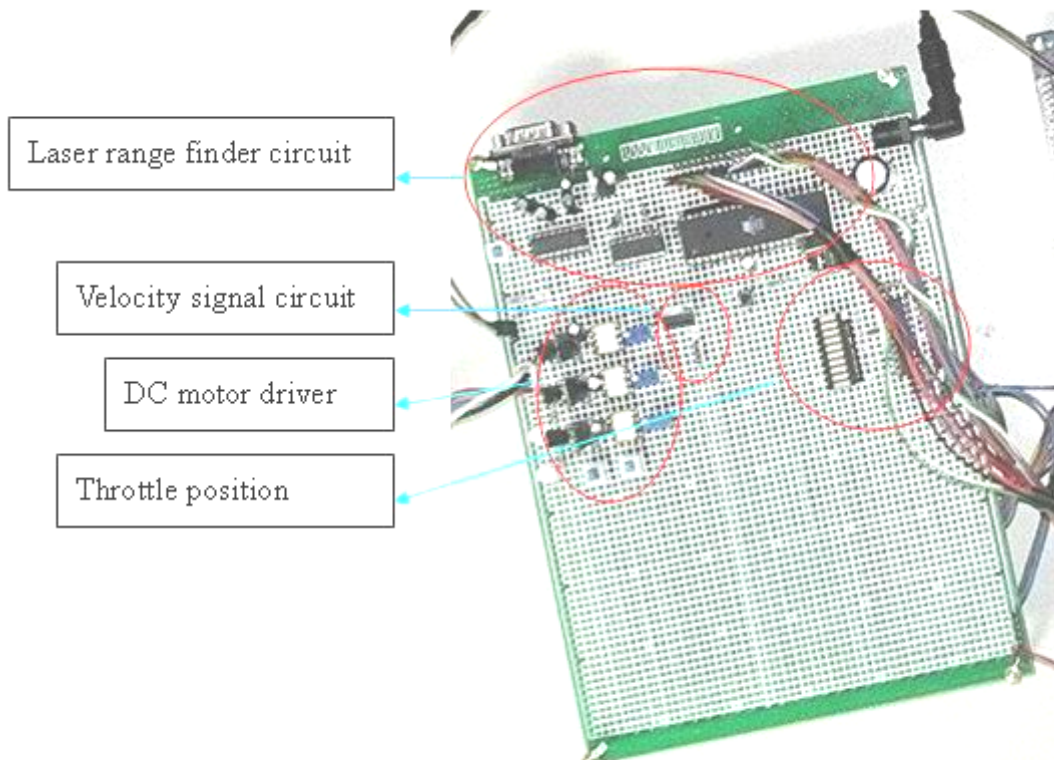
Figure 5-10 Interface circuit

5.3   Summary

5.3.1 Interface circuits

In this section, we show the experimental circuit in Figure 5-8 including the FPGA development board named EP1S25f780S5, interface circuit and the DC motor driving throttle. The detailed circuits are shown as Figure 5-9.

The blank space of the circuit is used to realize new functions if we want to upgrade our system or increase the display function that it can show the real velocity, desired velocity, real distance, desired distance or other we want to show in the interface circuit.

5.3.2 FPGA performance

Table 5-2 Overall performance of the FPGA

Total logic cells	4.429 / 25,660 (17%)
Total pins	79 /598 (13%)
Total memory bits	435 / 1,944,576 (< 1%)

Table 5-3 Comparison with all modules

Entity	Logic Cells	Memory Bits
Sensory processor	771	0
Supervisory I (before a_{des})	362	0
Supervisory II(a_{des} to v_{des})	1163	435
Regulation Control	1202	0
Peripheral	930	0

To achieve these objectives, the control platform closen in this work is based on a 25 k gate FPGA with 80 M Hz clock. Table 5-2 lists the used total logic cells, total pins and total memory bits. In detail, Table 5-3 lists the logic cells and the memory bits of all modules. It is known that the supervisory control II(a_{des} to v_{des}) occupies the depleted memory bits because it has a function like the integration used to compute the desired velocity from the desired acceleration and the real velocity. System input, the sensory processor, depletes 771 logic cells and it has a controversy. Here the ideal way to scant logic cells is used for verifying functions conveniently because we can test functions by MicroAutoBox in the same environment. It may have a lot of changes if we select the different sensory processor

Considering the FPGA based and PC based, the main reason of errors is from the difference between floating points and fixed points. This difference influences the desired velocity and the desired acceleration. By calculating, we estimate the maximum error of the desired velocity between FPGA based and PC based is about 1 km/hr and the maximum error of the desired acceleration between FPGA based and PC based is about 0.6 m/s^2.

One of solutions is to increase the total logic elements and the total memory bits for computing the decimal. An important source of errors is from the velocity signal decoding. Because of it, the performance between the FPGA based and PC based has an estimated error.

On the other hand, there is a problem in the supervisory control that we have no brake control. Because of it, the absolute of the maximum desired acceleration is bound in 2 m/s^2 that it is from the maximum acceleration when the vehicle decelerating without brake control.

Chapter 6   Conclusion

Integration of the human-in-the-loop design into a longitudinal automation design is presented in this paper, and the overall system is successfully implemented on a passenger vehicle tested in real road environments. The longitudinal automation system is composed of the adaptive sensory processor, the supervisory control, and the regulation control. The system safety is improved by inclusion of adaptive sensory scheme to prevent the missing detection of the preceding vehicle on curved roads. The supervisory control is designed to switch between different modes automatically and operate within the bound acceleration constraint without v-v communication need. The regulation control is to execute the desired velocity tracking commanded from the supervisory control. The proposed automation system is to assist the human driver in the velocity and inter-vehicle space control such as to yield the workload reduction of driving.

Finally, we proposed an FPGA-based autonomy adaptive cruise control system that has three modes including ICC, ACC and PLATOON mode. The greatest breakthrough of the system is a hierarchical design, supervisory control. It makes this system have variety. Through the desired distance, acceleration, velocity, and throttle position, we can reach our design goal. It makes the system can be expanded easily.

The focal point of this thesis is to implement the AACC system. In fact, the relation between experiment results with the forward looking sensor is very great. The distance information with the error will make our system unstable probably when meeting slopes or the other situations. In case of reality, the credibility of the real-time

distance information is depending on its scan range. Maybe it will be an important topic how to get the dependable distance information in the future.

Reference

[1] S. Huang, W. Ren, and S. C. Chan, "Design and performance evaluation of mixed manual and automated control traffic," *IEEE Trans. Systems, Man and Cybernetics Part: A*, vol. 30, no. 6, pp. 661-673, 2000.

[2] R. Parasuraman, T. B. Sheridan, and C. D. Wickens, "A model for types and levels of human interaction with automation," *IEEE Trans. Systems, Man and Cybernetics Part: A*, vol. 30, no. 3, pp. 286-297, 2000.

[3] A. Vahidi and A. Eskandarian, "Research advances in intelligent collision avoidance and adaptive cruise control," *IEEE Trans.   Intell. Transport. Syst.*, vol. 4, no. 3, pp. 143-153, 2003.

[4] H. Raza and P. Ioannou, "Vehicle following control design for automated highway systems," *IEEE Trans. Contr. Syst.*, pp. 43-60, 1996.

[5] R. Rajamani et al., "Design and experimental implementation of longitudinal control for a platoon of automated vehicles," *Trans. ASME J. Dyn. Syst. Meas. Contr.*, vol. 122, pp. 470-476, 2000.

[6] J. E. Naranjo et al, "Adaptive fuzzy control for inter-vehicle gap keeping," *IEEE Trans. Intell. Transport. Syst.*, vol. 4, no. 3, pp. 132-142, 2003.

[7] J. H. Kim et al, "Modeling of driver's collision avoidance maneuver based on controller switching model," *IEEE Trans. Systems, Man, and Cybernetics, Part: B*, vol. 35, no. 6, pp. 1131-1143, 2005.

[8] "ISO 2631/1: Mechanical Vibration and Shock-Evaluation of Human Exposure to Whole-body Vibration, Part 1. General Requirements," 1997.

[9] K. A. Unyelioglu, E. Hatipoglu, and U. Ozguner, "Design and stability analysis of a lane following controller," *IEEE Trans. Control Systems Technology*, vol. 5, no. 1, pp127-134, 1997.

[10] J. Y. Wong, *Theory of Ground Vehicles*, John Wiley & Sons, Inc., 2001.

[11] S. J. Wu et al, "The automated lane-keeping design for an intelligent vehicle," in *Proc. Intell. Veh. Symp. 2005*, Las Vegas, 2005, pp. 508-513.

[12] P. A. Ioannou and C. C. Chien, "Autonomous intelligent cruise control," *IEEE Trans. Veh. Technol.*, vol. 42, no. 4, pp. 657-672, 1993.

[13] B. J. Choi, S. W. Kwak, and B. K. Kim, "Design stability analysis of single-input fuzzy logic controller," *IEEE Trans. Syst. Man, and Cyber., Part: B*, vol. 30, no. 2, pp. 303-309, 2000.

[14] G. M. Takasaki and R. E. Fenton, "On the identification of vehicle longitudinal dynamics," *IEEE Trans. Automatic Control*, vol. AC-22, no. 4, pp. 610-615, 1977.

[15] A. S. Hauksdóttir and G. Sigurðardóttir, "On the use of robust design methods in vehicle longitudinal controller design," *ASME J. Dyna. Syst. Meas. and Contr.*, vol. 115, no. 3, pp.166-172, 1993.

[16] J. W. Perng, B. F. Wu, H. I. Chin, and T. T. Lee, "Limit cycle analysis of uncertain fuzzy vehicle control systems," in *Proc. IEEE Inter. Conf. Networking, Sensing, and Control*, Tucson, Arizona, 2005, pp. 626-631.

[17] A. V. Oppenheim, R. W. Schafer, and J. R. Buck, *Discrete-Time Signal Processing, 2nd Ed.*, Prentice-Hall, Inc., 1999.

[18] 中華汽車，中華汽車 SAVRIN 工作手冊。
http://team.caltech.edu/members/SICK/LMS_Quick_Manual_V1_1.pdf.

[19] BOSCH world wed site, http://www.bosch.com.

[20] Electric operated cruise control AP500 installation manual. http://www.autoalarm.ee/index.php?cruisecontrol.

[21] TOSHIB A photocoupler GaAlAs IRED & PHOTO-IC TLP250. http://www.toshiba.com/taec/components/Datasheet.

[22] Precision Pancake Load Cells, http://www.sensotec.com.

[23] 孫宗瀛、楊英魁，Fuzzy 控制 :理論、實作與應用，全華，民國八十七年。

[24] Altera world wed site, http://www.altera.com.

[25] W. H. Crouse, D. L. Anglin, 劉崇富 譯，汽車學(二)----汽車驅動系統與底盤，高立，台北，民國九十年。

[26] 林傳生，使用 VHDL 電路設計語言之數位電路設計，三版，儒林，台北，民國八十七年。

[27] 蔡朝陽，單晶片微電腦 8051/8951 原理與應用，五版，全華，台北，民國九十一年。